



HAL
open science

MoveFormer: a Transformer-based model for step-selection animal movement modelling

Ondřej Cífka, Simon Chamaille-Jammes, Antoine Liutkus

► To cite this version:

Ondřej Cífka, Simon Chamaille-Jammes, Antoine Liutkus. MoveFormer: a Transformer-based model for step-selection animal movement modelling. 2023. hal-04023957

HAL Id: hal-04023957

<https://hal.umontpellier.fr/hal-04023957>

Preprint submitted on 17 Oct 2023

HAL is a multi-disciplinary open access archive for the deposit and dissemination of scientific research documents, whether they are published or not. The documents may come from teaching and research institutions in France or abroad, or from public or private research centers.

L'archive ouverte pluridisciplinaire **HAL**, est destinée au dépôt et à la diffusion de documents scientifiques de niveau recherche, publiés ou non, émanant des établissements d'enseignement et de recherche français ou étrangers, des laboratoires publics ou privés.



Distributed under a Creative Commons Attribution 4.0 International License

MoveFormer: a Transformer-based model for step-selection animal movement modelling

Ondřej Cífka¹ Simon Chamaille-Jammes² Antoine Liutkus³

^{1,3}Zenith Team, LIRMM, CNRS UMR 5506, Inria, Univ Montpellier, France

²CEFE, CNRS, EPHE, IRD, Univ Montpellier, France

¹cifka@matfyz.cz

²simon.chamaille@cefe.cnrs.fr

³antoine.liutkus@inria.fr

Abstract

The movement of animals is a central component of their behavioural strategies. Statistical tools for movement data analysis, however, have long been limited, and in particular, unable to account for past movement information except in a very simplified way. In this work, we propose MoveFormer, a new step-based model of movement capable of learning directly from full animal trajectories. While inspired by the classical step-selection framework and previous work on the quantification of uncertainty in movement predictions, MoveFormer also builds upon recent developments in deep learning, such as the Transformer architecture, allowing it to incorporate long temporal contexts. The model predicts an animal's next movement step given its past movement history, including not only purely positional and temporal information, but also any available environmental covariates such as land cover or temperature. We apply our model to a diverse dataset made up of over 1550 trajectories from over 100 studies, and show how it can be used to gain insights about the importance of the provided context features, including the extent of past movement history. Our software, along with the trained model weights, is released as open source.

Contents

1	Introduction	3
2	Data	4
2.1	GPS location data	4
2.2	Taxon vectors	5
2.3	Geospatial variables	6
3	Model	7
3.1	Step-selection model	8
3.1.1	Input embeddings	8
3.1.2	Trajectory encoder	9
3.1.3	Candidate selection	9
3.1.4	Variable receptive field training	10
3.2	Data representation	10
3.2.1	Location	10
3.2.2	Time	10
3.2.3	Associated variables	11
3.3	Candidate sampling	11
3.4	Implementation details and hyperparameters	12
4	Analysis methods	12
4.1	Context length analysis	12
4.1.1	Relevant context length	13
4.1.2	Efficient evaluation	13
4.2	Candidate feature importance	14
5	Results	14
5.1	Validation	14
5.2	Context length analysis	15
5.3	Candidate feature importance	18
6	Discussion	19
7	Acknowledgments	20
A	Appendix	21

1 Introduction

The movement of animals is a central component of their behavioural strategies to best exploit the landscape they live in, to find a mate or to avoid predators, for instance. The role that these movements have beyond the individual, for instance in shaping animals' ecosystem impacts, is clear. Accordingly, and thanks to the technological developments that are allowing to collect more detailed movement data on more individuals and species each day, the study of animal movement has become an important goal of ecology [1].

For a long time, however, statistical tools to analyze movement data were lacking or limited. Over time, though, purely pattern-based descriptions (e.g. home-range analyses) have been complemented by regression models allowing to infer the effects of spatio-temporal features on movement. *Step-selection function* (SSF) models, which compare actual movement steps with realistic candidate ones, are one of such models and have de facto become the established approach to analyse animal trajectories [2–4]. They are now routinely used to infer and quantify the effect of environmental variables such as, for instance, land cover or temperature.

However, an animal's movement is likely to be driven not only by spatio-temporal environmental features, but also by some internal knowledge and rules that are unobservable directly. The importance of memory and of an animal's familiarity with places is increasingly recognized [5–7], and familiarity is usually incorporated into SSF models using a *previously visited* yes/no variable, or a *time-spent* variable, often calculated over an arbitrary time window [8, 9]. Memory of places and their characteristics can also lead to routine movement behaviours. Traplining, in which an individual travels to the same places in the same order, is rare, but it is clear from visual inspection of animal trajectories that many animals display some form of routine movement behaviours. But for traplining, which has received a lot of interest, the study of routine movement behaviour has remained extremely limited [10]. Riotte-Lambert et al. [11] showed how conditional entropy, calculated using the information on visits to patches, could be used as a metric of routine in movement. That metric has not been used much since then, possibly because the need to determine sites may render its application difficult on data collected in nature, where patches can be difficult to determine, be diffuse, or not exist at all. Further work is needed to describe and explain routine movements, which result from the interaction between memorized knowledge, movement rules and environmental context. Additionally, we are not aware of any work that has focused on how to incorporate complex information about past movement and environmental context into predictive models of animal movement, although it should, by definition, improve predictions. The question: 'To what extent past movements inform where an animal is likely to go next?' remains open.

The classic implementation of the SSF framework appears unsuitable to address this difficult question. We therefore developed a new type of model that we named MoveFormer. We conserved the conceptual attractiveness of SSF, but built on the most recent developments in deep learning to embed the information about current and past animal location, movement and environmental context.

Our contribution is threefold. First, we propose a model that learns to best predict the next step of a movement trajectory based on a given context length, i.e. a given time-window of information about the past. Second, the proposed

approach is flexible enough to allow each step in the context to be defined not only by the locations of the start and end points, but also by any kind of features that could be relevant, in particular environmental variables. Third, we show how the model can be used to gain insights about the importance of the provided context, both in terms of the extent of the past that it is useful to know, and in terms of what kinds of information are most ecologically relevant to predict an animal’s movement. We demonstrate this by comparing the predictions, via information-theoretic metrics and prediction accuracy, for different context lengths or with randomized features. Model training and analyses are conducted on a dataset made up of over 1550 trajectories from over 100 studies, encompassing various species within mammals, birds and reptiles.

The MoveFormer source code, including code for data pre-processing and evaluation, as well as complete hyperparameter settings, is available online.¹ We also release the weights of the trained models.²

2 Data

In this section, we describe our sources of data, specifically: movement data (trajectories consisting of latitudes, longitudes and timestamps), geospatial variables (associated with locations), and taxonomic classification information (associated with each animal).

2.1 GPS location data

Our main source of location data is Movebank³ [12], an online repository for animal movement data. The location data in Movebank is presented as latitude/longitude pairs along with UTC timestamps and is grouped into trajectories (*deployments*) and associated with (occasionally missing) metadata such as a taxon name, sex, and date of birth. We used the Movebank API to retrieve data from GPS sensors for all 269 studies that were available⁴ for download under a Creative Commons⁵ license (CC0, CC BY and CC BY-NC), obtaining 13 577 trajectories comprising a total of 197 million observations (location events). We subsampled the trajectories (splitting them into segments when necessary) so that observations occur at midnight and at noon (according to local mean time) with a tolerance of ± 3 h and so that the time difference between consecutive observations is 9 to 15 h. We discarded trajectory segments shorter than 120 observations, leaving us with 1440 trajectories from 98 different studies [13–165]. See Table 4 in the appendix for the full list of studies and their licenses.

We added unpublished data from 4 more studies, collected by one of us (S.C-J). These are GPS data from plains zebras and African elephants, collected in Hwange National Park (Zimbabwe), and GPS data from plains zebras and blue wildebeest, collected in Hluhluwe-iMfolozi Park (South Africa). After subsampling and filtering as in the case of the Movebank data, we obtained 73 trajectories.

¹<https://github.com/cifkao/moveformer>

²<https://doi.org/10.5281/zenodo.7698263>

³www.movebank.org

⁴as of 15 February 2022

⁵<https://creativecommons.org/>

section		#spec	#ind	#traj	#obs
train		61	1383	2786	915618
val		17	53	133	50984
test		21	70	133	40334
class	order	#spec	#ind	#traj	#obs
<i>Aves</i>		39	895	1915	640420
	Accipitriformes	10	138	315	65189
	Anseriformes	10	169	210	69386
	Bucerotiformes	1	5	6	4448
	Cathartiformes	1	12	34	8965
	Charadriiformes	10	310	585	235722
	Ciconiiformes	2	249	751	253541
	Gruiformes	1	1	1	189
	Passeriformes	1	3	3	474
	Pelecaniformes	1	6	6	1764
	Struthioniformes	1	1	1	221
	Suliformes	1	1	3	521
<i>Mammalia</i>		15	439	845	290789
	Artiodactyla	7	329	660	218698
	Carnivora	6	41	51	12404
	Perissodactyla	1	26	34	25582
	Proboscidea	1	43	100	34105
<i>Reptilia</i>		6	58	116	40353
	Testudines	6	58	116	40353

Table 1: Number of species, individuals, trajectories, and observations in each section of the dataset, and a breakdown by taxa.

The final dataset contains about 1 million observations from 1506 individuals, grouped into 1513 trajectories with a median length of 408. We performed a train/validation/test split, making sure that 1) the validation and test sections contain only frequent species (with at least 10 members in the full dataset), and 2) each individual appears in exactly one split. Table 1 details the amounts of data by section and by taxonomic classification and Fig. 1 shows the geographical distribution.

During training and evaluation, we additionally split each trajectory into segments of length $N_{\max} = 500$ and subsequently consider each of these segments as a separate trajectory.

2.2 Taxon vectors

Each trajectory in our data is associated with a taxon name (most commonly the animal’s species). To obtain a dense vector representation of the taxon, we look up its Wikipedia article and retrieve the associated 100-dimensional embedding vector from Wikipedia2Vec [166].

A property of Wikipedia2Vec is that embeddings of semantically similar entities are placed close together in the embedding space. To illustrate that this

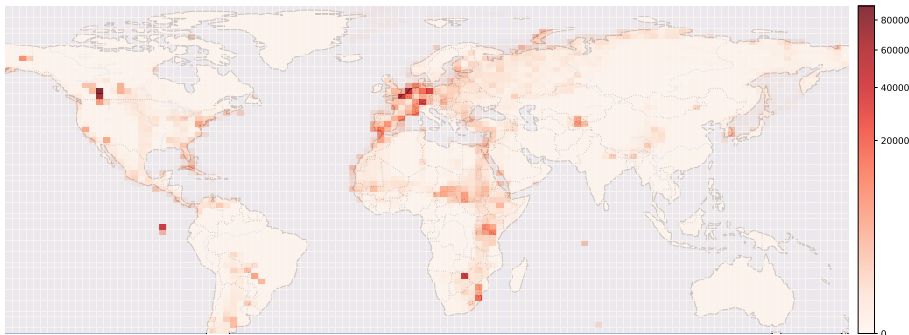


Figure 1: The geographical distribution of the observations in the dataset.

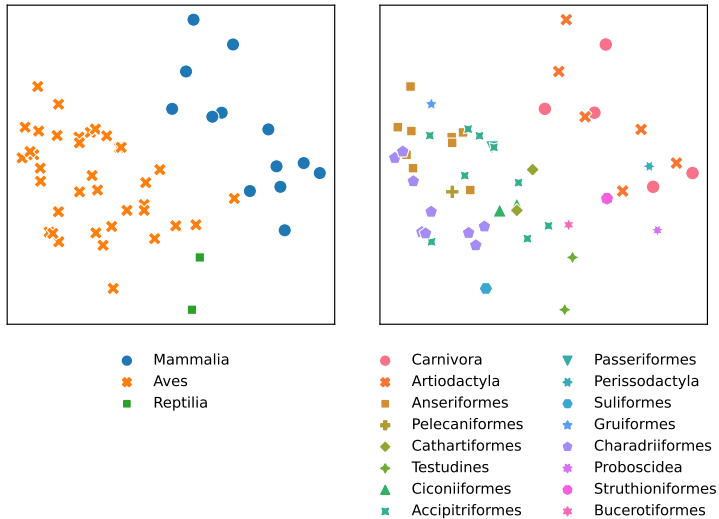


Figure 2: A PCA projection of Wikipedia2Vec embeddings of species, labeled by class (left) and order (right).

extends, to some degree, to similarity between species, we display in Fig. 2 the PCA (principal component analysis) projections of species embeddings, labeled by higher taxonomic ranks. We also measured the cosine similarity between all pairs of embeddings and found it to be correlated with the number of common ancestors of the two species in the taxonomic hierarchy (Spearman $\rho = 0.68$).

Overall, the Wikipedia2Vec embeddings appear to meaningfully encode a species' position in the phylogeny. Hence, we speculate (though we do not test this in the present work) that their inclusion in the model should help this model to generalize to species that are not present in the training data, at least as long as they are sufficiently similar to those that are.

2.3 Geospatial variables

The proposed model is powerful enough to account not only for each trajectory intrinsic dynamics but also for any *third-party* additional information that may

be available as covariates. In order to illustrate this, we augment each trajectory data point with exogenous information. For each location, we retrieve the following geospatial variables, which could be ecologically relevant, from publicly available raster data:

- 2009 Human Footprint, 2018 Release [167, 168] (resolution: ~ 1 km); we normalize the values between 0 and 1 and sample them with bilinear interpolation;
- 19 bioclimatic variables from WorldClim 2.1 [169] (resolution: ~ 1 km); we standardize the values (zero mean, unit variance) and use nearest neighbor interpolation;
- land cover classification (23 classes) from Copernicus Global Land Service, version 3.0.1, epoch 2015 [170] (resolution: ~ 100 m); we use a one-hot encoding and nearest neighbor interpolation.

3 Model

Formally, we consider the dataset as composed of *trajectories*, where a trajectory⁶ $\xi_{1\dots N}$ of length N consists of locations $x_{1\dots N}$, corresponding to timestamps $t_{1\dots N}$, and any associated variables $z_{1\dots N}$, i.e. $\xi_n = (x_n, z_n, t_n)$ as described above. Our main goal is to estimate a model for the next-step prediction task, i.e. for any given $n \in \{1, \dots, N\}$, predict the next location x_{n+1} from the trajectory prefix $\xi_{1\dots n}$ and the next timestamp t_{n+1} .

As a fundamental use case, we are interested in analyzing the effect of available past context on the prediction of x_{n+1} . Specifically, for a varying *context length* $c \in \{1, \dots, c_{\max}\}$ (where c_{\max} is an arbitrary constant), we wish to study the behavior of the prediction of x_{n+1} given $\xi_{n-c+1\dots n}$ and t_{n+1} . Hence, we are in fact interested in a model accepting as input any *trajectory segment* of length at most c_{\max} , and predicting the next location.

We adopt a step-selection function modelling approach [2, 4], based on selecting the end-point location of a step from a set of candidates. Specifically, for a position $n+1$ within a trajectory, given an associated timestamp t_{n+1} , a set of candidate locations $x_{n+1}^{(1\dots K)}$ and associated variables $z_{n+1}^{(1\dots K)}$, we are interested in estimating a probability distribution over the candidates:

$$P\left(y_{n+1} = i \mid \xi_{1\dots n}, t_{n+1}, x_{n+1}^{(1\dots K)}, z_{n+1}^{(1\dots K)}\right), \quad (1)$$

where $i \in \{1, \dots, K\}$.

We propose to model this distribution using a deep neural network, consisting of a *Transformer* [171] *encoder* and a *candidate selection module*, as depicted in Fig. 3. The role of the Transformer is to encode the trajectory up until position n , i.e. $\xi_{1\dots n}$ along with the timestamp for the next observation, t_{n+1} . The candidate selection module then encodes each candidate $x_{n+1}^{(i)}$ and employs an attention mechanism to compute a probability distribution over the candidates. The model is described in detail in Section 3.1, followed by our choice of input representation in Section 3.2.

⁶We use $\xi_{1\dots N}$ as shorthand notation for the sequence $\xi_1, \xi_2, \dots, \xi_N$. Note that N may be different for each trajectory in the dataset.

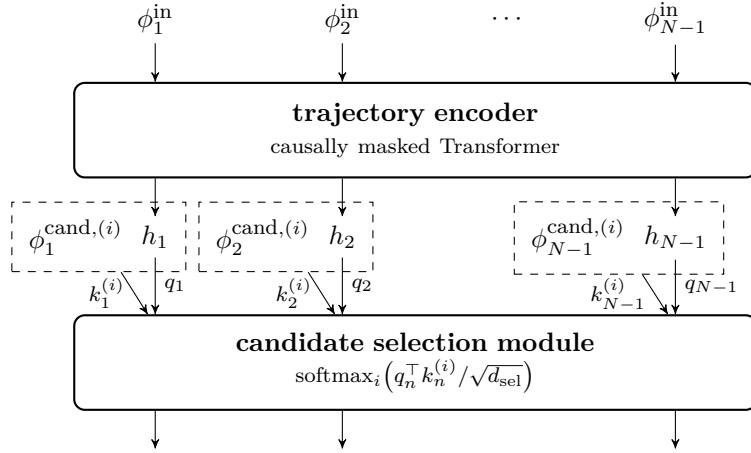


Figure 3: The high-level architecture of MoveFormer. The input to the trajectory encoder is a sequence of embedding vectors $\phi_{1\dots N-1}^{\text{in}}$, each corresponding to a different data point (location-timestamp pair) in the trajectory. The encoder outputs a sequence of vectors $h_{1\dots N-1}$; the causal masking in the encoder causes each h_n to encode only the inputs up to position n , i.e. $\phi_{1\dots n}^{\text{in}}$. This representation is then fed to the candidate selection module, which uses it as *queries* in an attention mechanism that assigns probabilities to different candidate locations. Both the input embeddings $\phi_{1\dots N-1}^{\text{in}}$ and the candidate embeddings $\phi_n^{\text{cand,(i)}}$ are computed through embedding layers which are not displayed here but described in Section 3.1.1.

In order to train and evaluate this model, we also need a way to generate suitable candidate locations $x_{n+1}^{(i)}$. We use a simple but general method employing quantile-based modelling of turning angles and movement distances, as detailed in Section 3.3.

3.1 Step-selection model

3.1.1 Input embeddings

We build two sets of embeddings $\phi_n^{\text{in}}, \phi_n^{\text{cand,(i)}} \in \mathbb{R}^{d_{\text{emb}}}$, $n \in \{1, \dots, N-1\}$, $i \in \{1, \dots, K\}$ such that:

- ϕ_n^{in} , input for the trajectory encoder, depends on $x_{n-1}, x_n, t_n, t_{n+1}, z_n$;
- $\phi_n^{\text{cand,(i)}}$, input for the candidate selection module, depends on $x_n, x_{n+1}^{(i)}, z_{n+1}^{(i)}$.

The inputs are represented as collections of carefully engineered continuous and discrete features that we will describe later (see Section 3.2). Missing (NaN) values are replaced with a special embedding vector learned as an additional parameter. In each case, we project each feature vector to a common embedding space $\mathbb{R}^{d_{\text{emb}}}$, then linearly combine them (with different learnable coefficients in each of the two cases).

More precisely, for ϕ^{in} :

$$\phi_n^{\text{in}} = \sum_{j=1}^F w^{\text{in},(j)} \left(W^{(j)} f_n^{(j)} + b^{(j)} \right), \quad (2)$$

where $f_n^{(j)}$ is the j -th out of all F feature vectors at step n , and the learnable parameters are coefficients $w^{\text{in},(j)} \in \mathbb{R}$ (we set $w^{\text{in},(j)} = 0$ for features we do not wish to consider), biases $b^{(j)} \in \mathbb{R}^{d_{\text{emb}}}$ and weight matrices $W^{(j)} \in \mathbb{R}^{d_{\text{emb}} \times d_j}$. The formula for $\phi_n^{\text{cand},(i)}$ is analogous. As can be seen from Eq. (2), the chosen method for constructing input embeddings allows features to have different dimensions and automatically projects them to the desired embedding dimension (via $W^{(j)}$ and $b^{(j)}$) before applying scaling through $w^{\text{in},(j)}$.

3.1.2 Trajectory encoder

The trajectory encoder is a Transformer encoder with causally masked attention. It receives the embedding sequence $\phi_{1\dots N-1}^{\text{in}}$ and outputs a sequence of vectors $h_{1\dots N-1}$ where h_n is a representation of $\xi_{1\dots n}$. The encoder does not use any positional encoding in the conventional sense (encoding the indices $1, \dots, N-1$, as is commonly done in Transformers), but position information is conveyed by the feature representations of the timestamps $t_{1\dots N-1}$.

3.1.3 Candidate selection

The candidate selection module is used to select the next location out of a list of candidates. We build upon the common approach that models the probability of an individual being present at a given candidate location via conditional logistic regression [3]; expressed in our notation:

$$\frac{\exp\left(\beta^\top \phi_n^{\text{cand},(i)}\right)}{\sum_{i'=1}^K \exp\left(\beta^\top \phi_n^{\text{cand},(i')}\right)}, \quad (3)$$

where β is a parameter vector.

In this work, in order to incorporate the context representation computed by the trajectory encoder, we replace the global parameter vector β with a context-dependent *query vector* $q_n \in \mathbb{R}^{d_{\text{sel}}}$, which is a linear projection of the trajectory encoder output h_n . We also do not use the raw candidate features $\phi_n^{\text{cand},(i)}$ but replace them with a *key vector* $k_n^{(i)} \in \mathbb{R}^{d_{\text{sel}}}$, which is computed by concatenating the feature vector with the corresponding encoder output h_n and passing the result through a *candidate encoder* (a fully-connected network): $k_n^{(i)} = E_{\text{cand}}([\phi_n^{\text{cand},(i)}, h_n])$. Thus, we arrive at a *dot-product attention mechanism*; scaling the dot products by $1/\sqrt{d_{\text{sel}}}$ as in Transformer attention [171], we have:

$$P\left(y_{n+1} = i \mid \xi_{1\dots n}, t_{n+1}, x_{n+1}^{(1\dots K)}, z_{n+1}^{(1\dots K)}\right) = \frac{\exp\left(q_n^\top k_n^{(i)} / \sqrt{d_{\text{sel}}}\right)}{\sum_{i'=1}^K \exp\left(q_n^\top k_n^{(i')} / \sqrt{d_{\text{sel}}}\right)}. \quad (4)$$

During training, the first candidate location $x_{n+1}^{(1)}$ is taken as the true next location x_{n+1} ; the rest of the candidates are randomly sampled around the current location x_n (we detail this process below). This allows us to define a cross entropy loss, which we minimize through stochastic gradient descent using the Adam optimizer:

$$\mathcal{L} = -\frac{1}{N-1} \sum_{n=1}^{N-1} \log_K P\left(y_{n+1} = 1 \mid \xi_{1\dots n}, t_{n+1}, x_{n+1}^{(1\dots K)}, z_{n+1}^{(1\dots K)}\right) \quad (5)$$

3.1.4 Variable receptive field training

As mentioned above, we aim to evaluate our model on arbitrary trajectory segments up to some maximum length c_{\max} (this procedure is detailed below in Section 4.1). As can be seen from Eq. (5), our model is effectively being simultaneously trained on all prefixes of the trajectory $\xi_{1\dots N}$. Hence, the model is able to accept segments of variable length as desired, but being only trained on trajectory prefixes may bias it, leading to incorrect predictions on segments that are not prefixes. To alleviate this, we propose a training scheme that intervenes on the attention weights to randomly vary the past context available for each prediction.

In each training batch, we sample a random integer B uniformly from $\{1, \dots, N_{\max}\}$ and apply a block-diagonal attention mask to the attention matrix (on top of the causal mask) with blocks of size B (with the last block truncated if $B \nmid N$). As a result, the ranges of positions $\{1, \dots, B\}$, $\{B+1, \dots, 2B\}$, etc. are prevented from attending to each other, and the corresponding segments are therefore effectively considered as separate trajectories.

3.2 Data representation

Let us now describe the feature mappings used for location and time, as well as associated features.

3.2.1 Location

In the raw data, each location x_n is represented as a GPS coordinate pair (latitude, longitude). We represent it as a geodetic normal vector (*n-vector*) $\nu(x_n) \in \mathbb{R}^3$.

Additionally, we encode the position relative to the previous location x_{n-1} as a *movement vector* $\mu(x_{n-1}, x_n) \in \mathbb{R}^2$, obtained by computing the bearing and distance from x_{n-1} to x_n and converting them to cartesian coordinates. We apply scaling to make the overall root-mean-square (RMS) of the norms of movement vectors computed on the training dataset equal to 1.

Analogously, we encode each candidate location $x_{n+1}^{(i)}$ as an n-vector $\nu(x_{n+1}^{(i)})$ and as a movement vector $\mu(x_n, x_{n+1}^{(i)})$.

3.2.2 Time

We encode a timestamp t_n as:

- a 10-dimensional vector of sines and cosines with a period of 1 second, 1 minute, 1 hour, 1 day, and 1 tropical (solar) year, respectively, such that their phase synchronizes on January 1st, 2000, at 00:00:00 UTC;
- $\sin(\text{LMT}/24 \cdot 2\pi)$ and $\cos(\text{LMT}/24 \cdot 2\pi)$, where LMT is the local mean time (i.e. UTC adjusted by longitude) in (fractional) hours;
- 3 integer values (one-hot-encoded) representing the calendar month (0–11), the day of the month (0–30), and the day of the week (0–6) in UTC.

We also encode the time difference w.r.t. the next timestamp t_{n+1} as a 12-dimensional vector of sines and cosines with the same periods as above, plus a period of 25 years. While this multi-scale encoding may not be necessary in our case (where the time differences are between 9 and 15 h), we propose it as a generic representation suitable for any time scale from seconds to years (and hence for virtually all existing animal movement data).

3.2.3 Associated variables

For each input and candidate location, we retrieve and pre-process geospatial variables as described in Section 2.3. We also include the taxon vectors (as described in Section 2.2) as an additional encoder feature vector for every element of the input sequence.

3.3 Candidate sampling

We sample each candidate location $x_{n+1}^{(i)}$ as follows:

- we estimate the current bearing β of the animal from the positions x_n and x_{n-1} ;
- we independently sample a *turning angle* $\theta \sim \hat{P}(\theta)$ and a *log-distance* $\log d \sim \hat{P}(\log d)$; $\beta' \leftarrow \beta + \theta$;
- we compute $x_{n+1}^{(i)}$ by moving x_n according to β' and d .

$\hat{P}(\theta)$ and $\hat{p}(\log d)$ are estimated on the training set as follows:

- We collect all turning angles from the training set and compute the quantiles (estimated using linear interpolation) at 101 equally spaced points $0 = q_0, q_1, \dots, q_{100} = 1$. We use them to construct the quantile function of $\hat{P}(\theta)$ as a piecewise linear function with knots at q_0, q_1, \dots, q_{100} .
- We collect the natural logarithms of all non-zero distances between consecutive points in the dataset; we construct the quantile function of $\hat{P}(\log d)$ analogously.

We sample from each distribution by drawing a sample from $\mathcal{U}[0, 1]$ and passing it through the estimated quantile function; this is sometimes called the *increasing rearrangement* [172].

In our experiments, we condition the distributions on the taxon, i.e. we estimate a separate pair of distributions on the section of the training dataset corresponding to each taxon.

3.4 Implementation details and hyperparameters

Our implementation of MoveFormer, available as open source software,⁷ is written in Python using the PyTorch framework⁸ and the `x-transformers`⁹ package. The code for efficient geospatial variable loading relies on the `rasterio`¹⁰ library and is released as a separate package, `gps2var`.¹¹

The trajectory encoder is a 6-layer Transformer with 8 attention heads per layer and a feature dimension of 128. The candidate encoder is a fully-connected neural network with one hidden layer of size 256 and a GELU activation [173]. The candidate selection module has $d_{\text{sel}} = 128$. The total number of parameters of the model is around 2.6 million – several orders of magnitude smaller than current state-of-the-art Transformer language models, for instance, but appropriate for the limited-size dataset that we are working with.

The Adam optimizer uses a learning rate of 5×10^{-5} with linear warm-up and exponential decay. We train for 180 epochs with a batch size of 24, taking 7.5 h on a Tesla V100 GPU (note that GPU utilization was only about 20 % and the performance bottleneck appeared to be the geospatial variable loading). We validate on the validation set twice per epoch and use the checkpoint with the lowest validation loss.

The complete hyperparameter settings are included with the source code.

4 Analysis methods

4.1 Context length analysis

Riotte-Lambert et al. [11] propose to use *conditional entropy* as a measure of uncertainty in predicting the next location given the c previous locations. Specifically, given a distribution P over sequences of locations, conditional entropy of order c can be written as

$$H_c = -\mathbb{E}_{P(s_1, \dots, s_c)}[\log P(s_{c+1} | s_1, \dots, s_c)], \quad (6)$$

where $P(s_1, \dots, s_c)$ is understood as the probability of c consecutive locations in a sequence being equal to s_1, \dots, s_c , and $P(s_{c+1} | s_1, \dots, s_c)$ as the conditional probability of s_{c+1} immediately following the sequence s_1, \dots, s_c . Considering this uncertainty measure as a function of the context length c , it may be used to study routine movement behavior.

Riotte-Lambert et al. [11] work with a finite set of discrete locations, allowing them to evaluate the expression (6) empirically on a given trajectory. However, the probability estimates quickly become unreliable with increasing c due to data sparsity. Moreover, the method is inapplicable when locations are unique, as in our case.

We propose an alternative way, which is to approximate $\log P$ using a suitable machine learning model (e.g. our proposed step selection model), so that

⁷<https://github.com/cifkao/moveformer>

⁸<https://pytorch.org/>

⁹<https://github.com/lucidrains/x-transformers>

¹⁰<https://github.com/rasterio/rasterio>

¹¹<https://github.com/cifkao/gps2var>

Eq. (6) becomes *cross entropy* computed on trajectory *segments* of appropriate length. In our case:¹²

$$\begin{aligned} H_c &\approx -\frac{1}{N-1} \sum_{n=1}^{N-1} \log_K P(y_{n+1} = 1 \mid \xi_{n-c+1\dots n}, t_{n+1}, x_{n+1}^{(1\dots K)}, z_{n+1}^{(1\dots K)}) \\ &= -\frac{1}{N-1} \sum_{n=1}^{N-1} \log_K P(y_{n+1} = 1 \mid \psi_{n,c}), \end{aligned} \quad (7)$$

where we collapse all the conditioning variables to $\psi_{n,c}$ for brevity. For more fine-grained analysis, we may be interested not in the sequence-level cross entropy, but rather in the “pointwise” values, i.e. $-\log_K P(y_{n+1} = 1 \mid \psi_{n,c})$.

More generally, we may alternatively choose to examine any metric that can be computed from the probabilities. We adopt the *relative entropy* (also known as the *Kullback-Leibler divergence*) of the prediction with the maximum context length c_{\max} with respect to the one at context length c (as proposed by Cifka and Liutkus [174] in the context of causal language models for text):

$$\begin{aligned} D_{\text{KL}}[P(y_{n+1} \mid \psi_{n,c_{\max}}) \parallel P(y_{n+1} \mid \psi_{n,c})] &= \\ &= \sum_{i=1}^K P(y_{n+1} = i \mid \psi_{n,c_{\max}}) \log \frac{P(y_{n+1} = i \mid \psi_{n,c_{\max}})}{P(y_{n+1} = i \mid \psi_{n,c})}. \end{aligned} \quad (8)$$

Note that this metric does not depend on the ground truth location, but measures the amount of information gained by considering the maximal context instead of the limited one.

4.1.1 Relevant context length

We may expect that there would be a critical context length C after which the above metrics stop improving, as further extending the context does not result in significant information gain. Similarly to Riotte-Lambert et al. [11], we define the *relevant context length* C_m – for a given metric m – as the smallest context length for which the metric reaches its optimum, with a 5% tolerance for robustness to noise:

$$C_m = \min \left\{ c: \frac{m(c) - \min_{c'} m(c')}{\max_{c'} m(c') - \min_{c'} m(c')} \leq 0.05 \right\}. \quad (9)$$

4.1.2 Efficient evaluation

We now discuss how to efficiently compute the probabilities needed to calculate the above metrics, following the procedure proposed for causal language models by Cifka and Liutkus [174]. We may collect all the probabilities in a tensor $\mathbf{P} \in \mathbb{R}^{N \times c_{\max} \times K}$ such that

$$\mathbf{P}_{n,c,i} = P(y_{n+1} = i \mid \psi_{n,c}). \quad (10)$$

Observe that by running the model on a segment of the trajectory corresponding to indices $n, \dots, n+c_{\max}-1$ for a given n , we obtain all the values $\mathbf{P}_{n+c-1,c,*}$ for

¹²We use the number of candidates K as the base of the logarithm for consistency with Eq. (5) and noting that this amounts to a multiplicative constant ($1/\log K$).

$c \in \{1, \dots, c_{\max}\}$. We may also notice that $\mathbf{P}_{n,n,*} = \mathbf{P}_{n,n+1,*} = \dots = \mathbf{P}_{n,c_{\max},*}$ for any $n < c_{\max}$. Hence, we can efficiently fill in the tensor \mathbf{P} using N runs of the model on segments of length at most c_{\max} .

4.2 Candidate feature importance

While the parameters of step-selection models fitted by conditional logistic regressions or point-process models are directly interpretable [4], deep learning models are known as “black boxes” that require special techniques to be interpreted post-hoc. A simple but popular technique [175, 176] is based on testing the model on a dataset with the values of a given feature randomly permuted. While aware of the caveats related to using this technique with correlated features [177], we employ it here to demonstrate the possibility of interpretation, and leave more advanced techniques for future work.

Specifically, we study how individual *candidate features* (components of $\phi_n^{\text{cand},(i)}$) influence the selection of candidates. We pick a feature (or a group of features), and for every observation in the dataset, we randomly shuffle the feature’s values among the K candidates (in contrast to Fisher et al. [176], who shuffle values across the entire dataset). The aim is to make the feature completely uninformative while maintaining its values plausible in the given context. We evaluate the model on both the permuted and the original dataset, and use the difference in performance as a measure of the importance of the selected feature.

5 Results

5.1 Validation

We evaluate the proposed model (here dubbed VARCTX) against variants to serve as baselines:

- FULLCTX is a variant without the variable receptive field training (see Section 3.1.4);
- NOATT is a model where all the attention layers are removed from the Transformer encoder, so that information is not allowed to flow between different positions in the sequence;
- NOENC is a model where the Transformer encoder is removed, i.e. we have $h_n = \phi_n^{\text{in}}$.

Note that the last two variants have a receptive field of 1 (i.e. only the features at position n are available for predicting the location at $n + 1$). To simulate this for VARCTX and FULLCTX in a comparable way, we test these in a regime (denoted by +DIAG) where the attention matrices are restricted to an identity matrix, i.e. each position can only attend to itself.

After running each of the above models on the test set, we compute the following metrics:

- xent@16: cross entropy (Eq. (5)) computed with 16 candidates;
- xent@100: cross entropy computed with 100 candidates;

model	xent@16 ↓	xent@100 ↓	acc 1/16 ↑	acc 10/100 ↑
FULLCTX	0.869	0.909	0.198	0.293
FULLCTX+DIAG	0.990	0.998	0.102	0.157
VARCTX	0.847	0.894	0.221	0.323
VARCTX+DIAG	0.932	0.954	0.136	0.204
NOATT	0.919	0.945	0.157	0.231
NOENC	0.928	0.950	0.148	0.217

Table 2: Results for different variants of the model. FULLCTX: trained on full trajectories (max. length 500); VARCTX: trained with variable receptive field; NOATT: no attention layers; NOENC: no encoder; DIAG: attention restricted to diagonal matrix during inference. Xent: cross entropy (lower is better), acc: accuracy (higher is better).

- acc 1/16: accuracy (i.e. how often the top scoring candidate is the ground truth) with 16 candidates,
- acc 10/100: top-10 accuracy (i.e. how often the ground truth is among the 10 top scoring candidates) with 100 candidates.

The results, averaged over all trajectories, are presented in Table 2. We note that the results are very consistent across all metrics, and we found all pairs of metrics to be strongly correlated (Pearson $\rho > 0.87$, computed over all models and trajectories).

Both FULLCTX and VARCTX outperform the rest of the models, which have a receptive field length of 1. This is evidence that providing past movement as context is beneficial. Interestingly, VARCTX yields better results than FULLCTX, possibly because the variable receptive field training scheme effectively makes the training data more diverse, alleviating overfitting.

We can also observe that the results of VARCTX+DIAG are closest to those of the models trained with minimum context (NOATT, NOENC). This suggests that the performance of VARCTX is not strongly degraded by limiting its receptive field at test time (unlike that of FULLCTX), validating our variable receptive field training approach.

Finally, we noticed large performance differences between species. For the VARCTX model, we calculated the average cross entropy for each taxonomic order (see Table 3) and found that it tends to be lower (i.e. better) for orders with a higher number of observations in the training set (Pearson $\rho = -0.71$).

5.2 Context length analysis

In this section, we demonstrate the ability to use the VARCTX to study the dependence of the predictions on the length c of the available past context, as described in Section 4.1. We set $c_{\max} = 200$ and $K = 16$.

First, we display in Fig. 5 the average cross entropy and relative entropy as a function of context length and by taxonomic order, and in Fig. 5 examples for concrete observations, with the relevant context length C highlighted. We observe that the best predictions tend to be achieved around context lengths 10–50, which corresponds to 5–25 days.

class	order	xent@16	#train
Aves	Accipitriformes	0.815	58 994
	Anseriformes	0.827	64 008
	Cathartiformes	1.057	8653
	Charadriiformes	0.815	205 602
	Ciconiiformes	0.697	237 304
Mammalia	Artiodactyla	0.928	201 464
	Carnivora	0.986	12 282
	Proboscidea	0.980	24 870
Reptilia	Testudines	0.998	34 577

Table 3: VARCTX validation cross entropies by taxonomic order, along with numbers of observations in the training data.

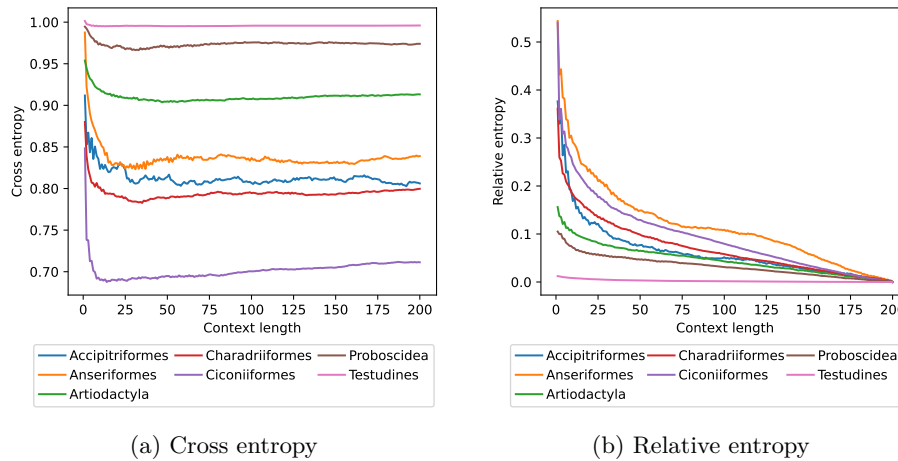


Figure 4: Metric value averages by context length and taxonomic order, computed on the test set (only positions $n > c_{\max} = 200$).

Apart from the clear inter-species differences in cross entropy already noted in the previous section (Table 3), we also observe some differences in *relative* entropy, though less marked. For example, while *Ciconiiformes*' movements are substantially easier (in terms of cross entropy) for our model to predict than those of *Anseriformes*, both have a similar relative entropy profile, indicating that the amount of information contributed by each time scale is similar for both taxa. On the other hand, note that the flat relative entropy profile of *Testudines* simply reflects a failure of our model to accurately predict their movements at any time scale – as evidenced by the cross entropy values being close to 1 –, which is possibly due to an insufficient amount of reptile training data.

Fig. 6 shows the distribution of the relevant context length C for each taxon in the test set. There are apparent differences between taxa, but we also note the large variability *within* each taxon that could be of interest in itself.

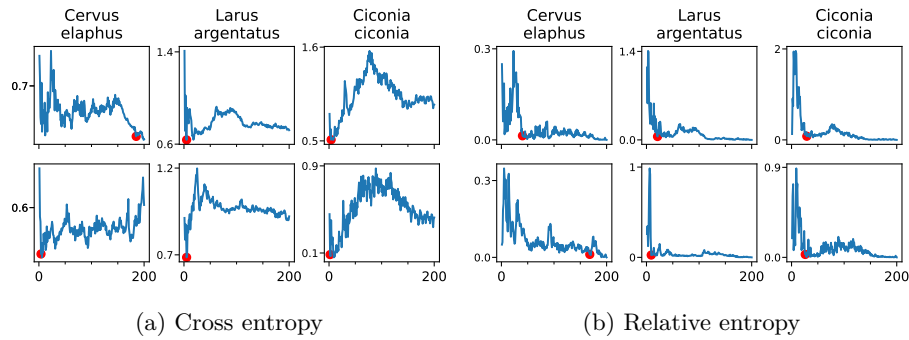


Figure 5: Examples of metric values (pointwise, i.e. for a single observation within a given trajectory) plotted as a function of context length. Top and bottom correspond to different (random) positions within the same trajectory. The red dot marks the relevant context length (where the metric reaches 5% of its min-max range).

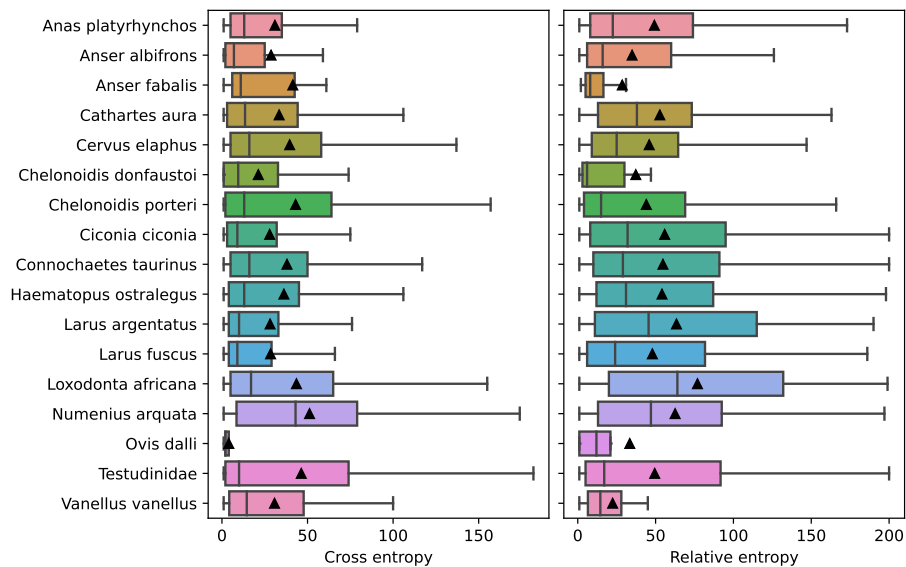


Figure 6: Relevant context length C by taxon, computed using cross entropy and relative entropy (pointwise values, as shown in Fig. 5), respectively. The black triangles indicate means.

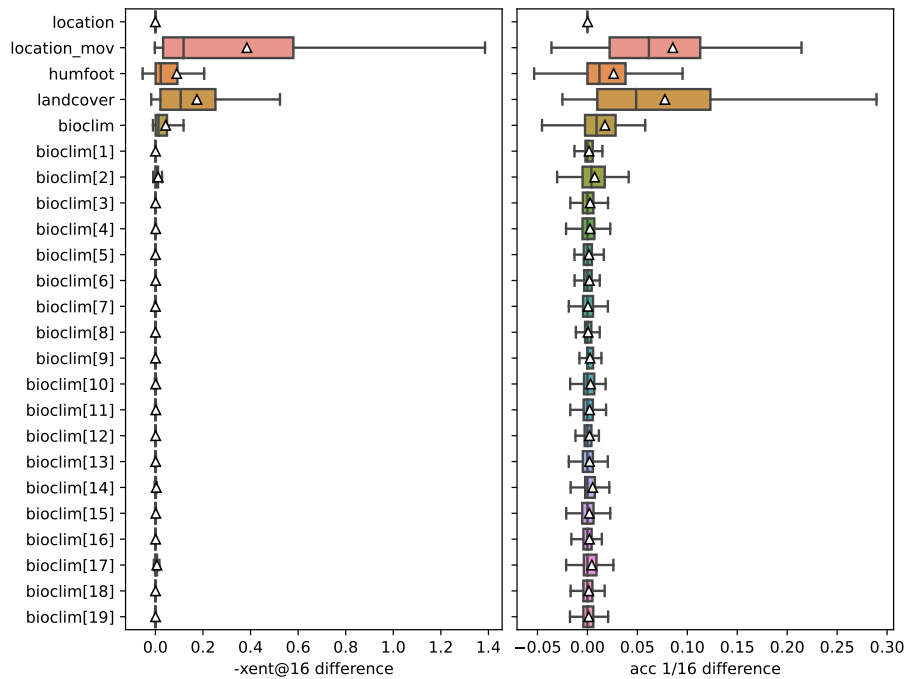


Figure 7: Candidate feature importances computed as differences between performance (measured using negative cross entropy and accuracy with 16 candidates) with and without permuted feature values. The plot shows the distribution over test trajectories. The features are, from top to bottom: location n-vector, movement vector, human footprint, land cover, and finally the 19 bioclimatic variables (BIO1 to BIO19), first as a group and then each individually.

5.3 Candidate feature importance

We present in Fig. 7 the results of the feature importance experiment. Vector features (location) are treated as groups; bioclimatic variables are tested both individually and as a group.

The most important features found by this method are movement vector and land cover, followed by human footprint. The bioclimatic variables appear to have relatively low impact, with the most important ones being BIO2 (mean diurnal range), BIO14 and BIO17 (both related to precipitation). Interestingly, global location (represented as n-vectors) seems to be the least important feature, possibly because it is difficult to exploit for candidate selection compared to the relative location information provided by the movement vectors.

Note that only *candidate* features $\phi_n^{\text{cand},(i)}$ are tested here, and the results do not say anything about the *input* (past observation) features $\phi_{1\dots n}^{\text{in}}$. For example, global location, which we found to be unimportant as a candidate feature, may well turn out to be an important past context feature.

6 Discussion

In this work, we propose a new model to learn from animal trajectories. Inspired by the classical step-selection framework [2] and previous work on the quantification of uncertainty in movement predictions [11], we designed MoveFormer, a step-based model of movement that builds upon recent developments in deep learning, such as the Transformer architecture. This allowed us to meet our initial goal to endow the model with a unique ability to learn how past movements influence current and future ones. Although this is an important question in movement ecology, it has remained poorly addressed so far because classical step-selection functions or other movements models are unable to account for past information except in a very simplified way (e.g. by including a feature indicating whether or not the animal has previously visited a given site).

An important contribution of this work is also to generalize the suggestion of Riotte-Lambert et al. [11] to use conditional entropy calculated over visits to discrete sites as a way to measure movement uncertainty. Although attractive, the difficulty of discretizing trajectories to meaningful ‘sites’ has slowed down the application of this idea. Here, we extend it to locations acquired in continuous space and propose cross-entropy and relative entropy, estimated through the movement model, as a more general approach. This allows to estimate the *relevant context length* (‘relevant order of dependency’ in Riotte-Lambert et al. [11]), i.e. the amount of the past that significantly improves the predictions about further movements. We did so in this study, and to the best of our knowledge, our study therefore provides the first estimation of how much of the past one needs to know to improve predictions of animal movements.

Our results suggest that for most datasets, predictions are improved when integrating the information from about a few days to two or three weeks before the movement to be predicted. Why this is the case, and why these results are broadly consistent between species, with possibly significant within-species variability, remains to be investigated further as it was beyond the goal of this methodological work. We note that, possibly, these results are affected by our choice to alternate sampling at midnight and at noon and to limit the length of trajectories to 500 locations, restricting the receptive field of our model to about 250 days. This may have weakened or excluded the influence of migration, which commonly leads to seasonal back-and-forth movement patterns and that, when accounted for, could help improve predictions about future movements.

One obvious limitation of our approach is the data requirement. As with all deep learning approaches, learning is limited by the data available in the training set, and enough data should also be available for validation and test sets. The whole dataset we gathered here, despite being rather large (> 1500 trajectories) compared to movement datasets currently analyzed in ecology, is likely close to the minimal size required to obtain a robust model and avoid severe overfitting issues. Currently, there are probably very few, if any, single-species datasets large enough to fit this model. For this reason, we aggregated data from numerous species; as a benefit, this allowed us to demonstrate that comparative analyses could be conducted with the model, for instance by comparing the distribution of relevant context lengths between species or higher-order taxa.

An important characteristic of the proposed approach is that the model not only accounts for past movements to predict new ones, but can also account for environmental predictors. First, this is crucial for realistic predictions, as the

step-selection literature has well demonstrated that step selection by animals is critically linked to habitats to be traversed or reached. Second, this allows to evaluate the relative importance of predictors in improving predictions. Interestingly, we found that purely relative positional information (movement vectors) could be more important than environmental variables for future location prediction. We tentatively suggest that this result might be linked to the fact that most animals favor familiar places and by doing so restrict themselves to well-established home-ranges [178]. We however also found, without surprise, that among the environmental variables tested, land cover and human footprint significantly affected animal movements [179].

To summarize, in the present work, we provide a new, state-of-the art model to analyze and predict animal movement data. The novelty of the model lies in the fact that it leverages the power of deep learning approaches and can account for past movements in the predictions. However, we emphasize, and have shown above, that the model is not only a tool for prediction, but can also be used to test hypotheses about the intrinsic and extrinsic drivers of animal movements.

7 Acknowledgments

This work was supported by the LabEx NUMEV (ANR-10-LABX-0020) and the REPOS project, both funded by the I-Site MUSE (ANR-16-IDEX-0006). Computations were performed using HPC/AI resources from GENCI-IDRIS (Grant AD011012019R1).

We would like to thank all authors who made their data available through MoveBank under Creative Commons licenses (see Table 4 in the appendix for the list of datasets used in this work).

A Appendix

Table 4: The list of all Movebank datasets used in this work.

ID	Name and references	License
446579	MPIAB Lake Constance Mallards GPS [13]	CC BY
481458	Vultures Acopian Center USA GPS [14–17]	CC BY
1764627	Kruger African Buffalo, GPS tracking, South Africa [18–21]	CC0
2928116	Galapagos Tortoise Movement Ecology Programme [22–28]	CC BY
2988333	Navigation experiments in lesser black-backed gulls (data from Wikelski et al. 2015) [29, 30]	CC0
6770990	MPIAB PNIC hurricane frigate tracking [127]	CC BY
7002955	HUJ MPIAB White Stork GSM E-Obs [128]	CC BY
7431347	MPIAB Argos white stork tracking (1991-2018) [31]	CC BY
8019591	Dunn Ranch Bison Tracking Project [129]	CC BY
8849813	LifeTrack - Great Egrets [130]	CC0
8863543	HUJ MPIAB White Stork E-Obs [131]	CC BY
9493881	LifeTrack White Stork Uzbekistan [132]	CC BY
9651291	Egyptian vultures in the Middle East and East Africa [32–35]	CC BY
10157679	LifeTrack White Stork Tunisia [133]	CC BY
10204361	Pandion haliaetus Osprey - SouthEast Michigan [134]	CC0
10236270	LifeTrack White Stork Armenia [36–38]	CC BY
10449318	LifeTrack White Stork Loburg [135]	CC BY
10449535	LifeTrack White Stork Greece Evros Delta [36–38]	CC BY
10449698	HUJ MPIAB White Stork GSM 2013 [136]	CC BY
10596067	LifeTrack White Stork Moscow [36–38]	CC BY
10763606	LifeTrack White Stork Poland [37]	CC BY
14671003	Hooded Vulture Africa [137]	CC BY
16880941	Turkey vultures in North and South America (data from Dodge et al. 2014) [17, 39]	CC0
19411459	Movement ecology of the jaguar in the largest floodplain of the world, the Brazilian Pantanal [40–45]	CC0
20202974	e-Obs GPRS Himalayan Griffon - Bhutan-MPIAB [46–49]	CC BY
21231406	LifeTrack White Stork SW Germany [37, 38, 50, 51]	CC BY
24442409	LifeTrack White Stork Bavaria [38, 50, 52]	CC BY
69724677	FTZ Geese Wadden Sea [138]	CC0
74496970	MPIAB white stork lifetime tracking data (2013-2014) [36, 37, 53]	CC BY
92261778	LifeTrack Whooper Swan Latvia [139]	CC BY
133992043	Migration timing in white-fronted geese (data from Kölzsch et al. 2016) [54, 55]	CC BY
173641633	LifeTrack White Stork Vorarlberg [50, 56]	CC BY
178979729	Latham Alberta Wolves [57, 58]	CC BY-NC
178994931	Peters Hebblewhite Alberta-BC Moose [59]	CC BY
182746263	High-altitude flights of Himalayan vultures (data from Sherub et al. 2016) [47, 49]	CC0
190490326	Movement strategies of Galapagos tortoises (data from Bastille-Rousseau et al. 2016) [24, 26–28]	CC BY-NC
208413731	White-bearded wildebeest in Kenya [60]	CC BY
209824313	Hebblewhite Alberta-BC Wolves [61, 62]	CC BY
212096177	LifeTrack White Stork Oberschwaben [38, 50, 63]	CC BY
217784323	Vultures Acopian Center USA 2003-2016 [16, 17, 64]	CC BY
236953686	LifeTrack Ducks Lake Constance [140]	CC0
329155299	Canada geese (<i>Branta canadensis</i>) [141]	CC0
384868221	White-tailed Eagle Poland. [142]	CC BY-NC
475878514	Coyote Valley Bobcat Habitat Connectivity Study [143]	CC BY-NC

Continued on next page

Table 4: The list of all Movebank datasets used in this work. (Continued)

ID	Name and references	License
501787846	Aromas Hills Bobcat Habitat Connectivity Study [144]	CC BY-NC
505156776	Graugans Zugverhalten Neusiedler See [145]	CC BY-NC
560041066	Eastern flyway spring migration of adult white storks (data from Rotics et al. 2018) [65, 66]	CC BY
604806671	MH_WATERLAND - Western marsh harriers (<i>Circus aeruginosus</i> , Accipitridae) breeding near the Belgium-Netherlands border [67]	CC0
657674643	North Sea population tracks of greater white-fronted geese 2014-2017 (data from Kölzsch et al. 2019) [68, 69]	CC BY
657965212	Pannonic population tracks of greater white-fronted geese 2013-2017 (data from Kölzsch et al. 2019) [69, 70]	CC BY
672882373	Milvus_milvus_atlantismarcuard [146]	CC BY-NC
673728219	NPS Dall Sheep in Yukon-Charley Rivers National Preserve [147]	CC BY
736029750	ThermochronTracking Elephants Kruger 2007 [71, 72]	CC BY-NC
892924356	Milvus migrans [148]	CC0
897981076	Ya Ha Tinda elk project, Banff National Park, 2001-2020 (females) [61, 62, 73–78]	CC0
918219824	ECOPATH, Brown skua, Boulinier et al., Amsterdam Island [149]	CC BY-NC
922263102	H_GRONINGEN - Western marsh harriers (<i>Circus aeruginosus</i> , Accipitridae) breeding in Groningen (the Netherlands) [79]	CC0
933711994	Elk in southwestern Alberta [80–91]	CC BY
938783961	MH_ANTWERPEN - Western marsh harriers (<i>Circus aeruginosus</i> , Accipitridae) breeding near Antwerp (Belgium) [92]	CC0
985143423	LBBG_ZEEBRUGGE - Lesser black-backed gulls (<i>Larus fuscus</i> , Laridae) breeding at the southern North Sea coast (Belgium and the Netherlands) [93]	CC0
986040562	HG_OOSTENDE - Herring gulls (<i>Larus argentatus</i> , Laridae) breeding at the southern North Sea coast (Belgium) [94]	CC0
1030734949	Biotelemetry of Bewick's swans [95, 96]	CC0
1049685237	Greater white-fronted goose family migration flight [97, 98]	CC0
1071134107	Herring Gulls (<i>Larus Argentatus</i>); Ronconi; Brier Island, Canada [99, 100]	CC0
1077731101	Eurasian Curlews [ID_PROG 1083] [150]	CC BY-NC
1080341217	Herring Gulls (<i>Larus Argentatus</i>); Clark; Massachussets, United States [100, 101]	CC0
1080341737	Herring Gulls (<i>Larus Argentatus</i>); Ronconi; Sable Island, Canada [100, 102]	CC0
1087068449	Von der Decken's hornbill (Jetz Kenya) [103, 104]	CC0
1088836380	Carnivore movements near Black Rock Forest New York [151]	CC BY
1091848505	gullSpecies_USGS_ASC_argosGPS [105]	CC0
1092737859	GPS calibration data (global) [152]	CC BY
1099562810	O_WESTERSCHELDE - Eurasian oystercatchers (<i>Haematopus ostralegus</i> , Haematopodidae) breeding in East Flanders (Belgium) [106]	CC0
1123149708	Ivory gull N Greenland 2018/19 [153]	CC BY-NC
1208105916	Caspian Gulls - Poland [154]	CC0
1229945587	Common Crane 2020 (Lithuanian University of Educational Studies; LEU) [155]	CC0
1241071371	Arctic fox Bylot - GPS tracking [156]	CC0
1259686571	LBBG_JUVENILE - Juvenile lesser black-backed gulls (<i>Larus fuscus</i> , Laridae) hatched in Zeebrugge (Belgium) [107]	CC0
1260886163	Cheetah Pilanesberg National Park, South Africa, 2014-2015 [108, 109]	CC0
1266784970	Corvus corone [ID_PROG 883] [157]	CC BY-NC

Continued on next page

Table 4: The list of all Movebank datasets used in this work. (Continued)

ID	Name and references	License
1278021460	BOP_RODENT - Rodent specialized birds of prey (Circus, Asio, Buteo) in Flanders (Belgium) [110]	CC0
1285079529	Monitoring of Capra ibex (Bovidae) populations in the western alps (project ALCOTRA LEMED-IBEX) [158]	CC BY
1393954358	Cathartes aura MPIAB Cuba [159]	CC BY-NC
1395952585	FTZ: Migrating curlews (data from Schwemmer et al. 2021) [111, 112]	CC0
1410035327	HUJ MPIAB White Stork E-Obs (subset for Carlson et al. 2021) [113, 114]	CC0
1415844328	Moult migration of taiga bean geese to Novaya Zemlya [115, 116]	CC BY
1448377103	Wood stork (Mycteria americana) Southeastern US 2004-2019 [117, 118]	CC0
1448409403	Lapwing NFW Vanellus Vanellus [160]	CC BY-NC
1498452485	Variability of White Stork flight patterns prior to earthquakes [161]	CC0
1562253659	LifeTrack White Stork Sarralbe [ID_PROG 1093] [162]	CC0
1605798640	O_BALGZAND - Eurasian oystercatchers (Haematopus ostralegus, Haematopodidae) wintering on Balgzand (the Netherlands) [119]	CC0
1605799506	O_SCHIERMONNIKOOG - Eurasian oystercatchers (Haematopus ostralegus, Haematopodidae) breeding on Schiermonnikoog (the Netherlands) [120]	CC0
1605802367	O_VLIELAND - Eurasian oystercatchers (Haematopus ostralegus, Haematopodidae) breeding and wintering on Vlieland (the Netherlands) [121]	CC0
1605803389	O_AMELAND - Eurasian oystercatchers (Haematopus ostralegus, Haematopodidae) breeding on Ameland (the Netherlands) [122]	CC0
1606812667	Hawksbill/green turtles Chagos Archipelago Western Indian Ocean [123, 124]	CC0
1671751878	Tchad Redneck Ostrich [163]	CC BY-NC
1841261165	Eurasian wigeon (Mareca penelope) Netherlands Lithuania 2018-2019 [125, 126]	CC BY
1907973121	Lowland tapirs, Tapirus terrestris, in Southern Brazil [164]	CC BY-NC
1907974323	Vega gull (Larus vegae) - GPS - Russia South Korea Japan [165]	CC BY-NC

class	order	taxon	#obs			
			train	val	test	
Aves	Accipitriformes	Cathartes aura	37609	2186	1703	
		Circus aeruginosus	5537	—	—	
		Circus cyaneus	540	—	—	
		Circus pygargus	1088	—	—	
		Gyps himalayensis	4047	736	312	
		Haliaeetus albicilla	409	—	—	
		Milvus milvus	323	—	—	
		Necrosyrtes monachus	4337	951	126	
		Neophron percnopterus	2138	—	—	
		Pandion haliaetus	2966	181	—	
		Anseriformes	Anas penelope	8297	—	—
			Anas platyrhynchos	22207	1970	1484
	Anser albifrons		18871	1122	558	
	Anser anser		3549	—	—	
	Anser fabalis		6258	—	244	
	Anseriformes		1123	—	—	
	Branta bernicla		1566	—	—	
	Branta leucopsis		628	—	—	
	Cygnus columbianus		602	—	—	
	Cygnus cygnus		907	—	—	
	Bucerotiformes	Tockus deckeni	4448	—	—	
	Cathartiformes	Coragyps atratus	8653	—	312	
	Charadriiformes	Haematopus ostralegus	44582	5439	3960	
		Larus	196	—	—	
		Larus argentatus	39655	8237	909	
		Larus cachinnans	1021	—	—	
		Larus fuscus	91380	8202	1534	
		Larus glaucescens	293	—	—	
		Larus smithsonianus	900	—	—	
		Larus vegae	10018	—	—	
		Numenius arquata	14896	—	1588	
		Vanellus vanellus	2661	—	251	
Ciconiiformes		Ciconia ciconia	230170	5835	10402	
		Mycteria americana	7134	—	—	
Gruiformes	Grus grus	189	—	—		
Passeriformes	Corvus corone	474	—	—		
Pelecaniformes	Ardea alba	1764	—	—		
Struthioniformes	Struthio camelus	221	—	—		
Suliformes	Fregata magnificens	521	—	—		
Mammalia	Artiodactyla	Alces alces	3061	—	—	
		Bison bison	130	—	—	
		Cervus elaphus	158108	6648	3849	
		Connochaetes taurinus	30036	755	4065	
		Ovis dalli	9075	934	983	
		Sus scrofa	556	—	—	
		Syncerus caffer	498	—	—	
		Acinonyx jubatus	239	—	—	
		Canis lupus	4811	—	122	
		Lynx	426	—	—	
	Carnivora	Lynx rufus	4353	—	—	
		Panthera onca	1873	—	—	
		Vulpes lagopus	580	—	—	
		Equus quagga	24873	709	—	
		Perissodactyla	Loxodonta africana	24870	5696	3539
			Testudines	Chelonoidis	546	—
		Chelonoidis donfaustoi		9386	594	251
		Chelonoidis hoodensis		2251	—	—
Chelonoidis porteri	12560	789		2283		
Eretmochelys imbricata	1286	—		—		
Testudinidae	8548	—		1859		
Reptilia	Testudines	Chelonoidis	546	—	—	
		Chelonoidis donfaustoi	9386	594	251	
		Chelonoidis hoodensis	2251	—	—	
		Chelonoidis porteri	12560	789	2283	
		Eretmochelys imbricata	1286	—	—	
		Testudinidae	8548	—	1859	

Table 5: Number of observations of each taxon in each section of the dataset.

References

- [1] Roland Kays, Margaret C. Crofoot, Walter Jetz, and Martin Wikelski. Terrestrial animal tracking as an eye on life and planet. *Science*, 348(6240): aaa2478, 2015. Publisher: American Association for the Advancement of Science.
- [2] Henrik Thurfjell, Simone Ciuti, and Mark S. Boyce. Applications of step-selection functions in ecology and conservation. *Movement ecology*, 2:1–12, 2014. Publisher: Springer.
- [3] Tal Avgar, Jonathan R. Potts, Mark A. Lewis, and Mark S. Boyce. Integrated step selection analysis: bridging the gap between resource selection and animal movement. *Methods in Ecology and Evolution*, 7(5):619–630, 2016. ISSN 2041-210X. doi: 10.1111/2041-210X.12528. URL <https://onlinelibrary.wiley.com/doi/abs/10.1111/2041-210X.12528>.
- [4] John Fieberg, Johannes Signer, Brian Smith, and Tal Avgar. A ‘How to’ guide for interpreting parameters in habitat-selection analyses. *Journal of Animal Ecology*, 90(5):1027–1043, 2021. ISSN 1365-2656. doi: 10.1111/1365-2656.13441. URL <https://onlinelibrary.wiley.com/doi/abs/10.1111/1365-2656.13441>.
- [5] William F. Fagan, Mark A. Lewis, Marie Auger-Méthé, Tal Avgar, Simon Benhamou, Greg Breed, Lara LaDage, Ulrike E. Schlägel, Wen-wu Tang, and Yannis P. Papastamatiou. Spatial memory and animal movement. *Ecology letters*, 16(10):1316–1329, 2013. Publisher: Wiley Online Library.
- [6] Louise Riotte-Lambert, Simon Benhamou, and Simon Chamaillé-Jammes. How memory-based movement leads to nonterritorial spatial segregation. *The American Naturalist*, 185(4):E103–E116, 2015. Publisher: University of Chicago Press Chicago, IL.
- [7] Nathan Ranc, Paul R. Moorcroft, Federico Ossi, and Francesca Cagnacci. Experimental evidence of memory-based foraging decisions in a large wild mammal. *Proceedings of the National Academy of Sciences*, 118(15): e2014856118, 2021. Publisher: National Acad Sciences.
- [8] Luiz Gustavo R. Oliveira-Santos, James D. Forester, Ubiratan Pivezan, Walfrido M. Tomas, and Fernando A. S. Fernandez. Incorporating animal spatial memory in step selection functions. *Journal of Animal Ecology*, 85(2):516–524, 2016. ISSN 1365-2656. doi: 10.1111/1365-2656.12485. URL <https://onlinelibrary.wiley.com/doi/abs/10.1111/1365-2656.12485>. [_eprint: https://besjournals.onlinelibrary.wiley.com/doi/pdf/10.1111/1365-2656.12485](https://besjournals.onlinelibrary.wiley.com/doi/pdf/10.1111/1365-2656.12485).
- [9] Jerod A. Merkle, Hall Sawyer, Kevin L. Monteith, Samantha PH Dwinell, Gary L. Fralick, and Matthew J. Kauffman. Spatial memory shapes migration and its benefits: evidence from a large herbivore. *Ecology letters*, 22(11):1797–1805, 2019. Publisher: Wiley Online Library.

- [10] Oded Berger-Tal and Shirli Bar-David. Recursive movement patterns: review and synthesis across species. *Ecosphere*, 6(9):art149, 2015. ISSN 2150-8925. doi: 10.1890/ES15-00106.1. URL <https://onlinelibrary.wiley.com/doi/abs/10.1890/ES15-00106.1>. eprint: <https://esajournals.onlinelibrary.wiley.com/doi/pdf/10.1890/ES15-00106.1>.
- [11] Louise Riotte-Lambert, Simon Benhamou, and Simon Chamaillé-Jammes. From randomness to traplining: a framework for the study of routine movement behavior. *Behavioral Ecology*, 28(1):280–287, January 2017. ISSN 1045-2249. doi: 10.1093/beheco/arw154. URL <https://doi.org/10.1093/beheco/arw154>.
- [12] Roland Kays, Sarah C. Davidson, Matthias Berger, Gil Bohrer, Wolfgang Fiedler, Andrea Flack, Julian Hirt, Clemens Hahn, Dominik Gauggel, Benedict Russell, Andrea Kölzsch, Ashley Lohr, Jesko Partecke, Michael Quetting, Kamran Safi, Anne Scharf, Gabriel Schneider, Ilona Lang, Friedrich Schaeuffelhut, Matthias Landwehr, Martin Storhas, Louis van Schalkwyk, Candace Vinciguerra, Rolf Weinzierl, and Martin Wikelski. The Movebank system for studying global animal movement and demography. *Methods in Ecology and Evolution*, 13(2):419–431, 2022. ISSN 2041-210X. doi: 10.1111/2041-210X.13767. URL <https://onlinelibrary.wiley.com/doi/abs/10.1111/2041-210X.13767>. <https://onlinelibrary.wiley.com/doi/pdf/10.1111/2041-210X.13767>.
- [13] Pius Korner, Annette Sauter, Wolfgang Fiedler, and Lukas Jenni. Variable allocation of activity to daylight and night in the mallard. *Animal Behaviour*, 115:69–79, may 2016. doi: 10.1016/j.anbehav.2016.02.026. URL <https://doi.org/10.1016/j.anbehav.2016.02.026>.
- [14] Keith L. Bildstein, David Barber, Marc J. Bechard, Maricel Graña Grilli, and Jean-François Therrien. Data from: Study "Vultures Acopian Center USA GPS" (2003-2021), 2021. URL <https://www.doi.org/10.5441/001/1.f3qt46r2>.
- [15] Julie M. Mallon, Keith L. Bildstein, and William F. Fagan. Inclement weather forces stopovers and prevents migratory progress for obligate soaring migrants. *Movement Ecology*, 9(1), jul 2021. doi: 10.1186/s40462-021-00274-6. URL <https://doi.org/10.1186/s40462-021-00274-6>.
- [16] Maricel Graña Grilli, Sergio A. Lambertucci, Jean-François Therrien, and Keith L. Bildstein. Wing size but not wing shape is related to migratory behavior in a soaring bird. *Journal of Avian Biology*, 48(5):669–678, mar 2017. doi: 10.1111/jav.01220. URL <https://doi.org/10.1111/jav.01220>.
- [17] Somayeh Dodge, Gil Bohrer, Keith Bildstein, Sarah C. Davidson, Rolf Weinzierl, Marc J. Bechard, David Barber, Roland Kays, David Brandes, Jiawei Han, and Martin Wikelski. Environmental drivers of variability in the movement ecology of turkey vultures (*Cathartes aura*) in North and South America. *Philosophical Transactions of the Royal Society B:*

- Biological Sciences*, 369(1643):20130195, may 2014. doi: 10.1098/rstb.2013.0195. URL <https://doi.org/10.1098/rstb.2013.0195>.
- [18] Paul C. Cross, Justin A. Bowers, Craig T. Hay, Julie Wolhuter, Peter Buss, Markus Hofmeyr, Johan T. Du Toit, and Wayne M. Getz. Data from: Nonparameteric kernel methods for constructing home ranges and utilization distributions, 2016. URL <https://www.doi.org/10.5441/001/1.j900f88t>.
- [19] Justin M. Calabrese, Chris H. Fleming, and Eliezer Gurarie. ctmm: an r package for analyzing animal relocation data as a continuous-time stochastic process. *Methods in Ecology and Evolution*, 7(9):1124–1132, may 2016. doi: 10.1111/2041-210x.12559. URL <https://doi.org/10.1111/2041-210x.12559>.
- [20] P. C. Cross, D. M. Heisey, J. A. Bowers, C. T. Hay, J. Wolhuter, P. Buss, M. Hofmeyr, A. L. Michel, R. G. Bengis, T. L. F. Bird, J. T. Du Toit, and W. M. Getz. Disease, predation and demography: assessing the impacts of bovine tuberculosis on African buffalo by monitoring at individual and population levels. *Journal of Applied Ecology*, 46(2):467–475, apr 2009. doi: 10.1111/j.1365-2664.2008.01589.x. URL <https://doi.org/10.1111/j.1365-2664.2008.01589.x>.
- [21] Wayne M. Getz, Scott Fortmann-Roe, Paul C. Cross, Andrew J. Lyons, Sadie J. Ryan, and Christopher C. Wilmers. LoCoH: Nonparameteric kernel methods for constructing home ranges and utilization distributions. *PLoS ONE*, 2(2):e207, feb 2007. doi: 10.1371/journal.pone.0000207. URL <https://doi.org/10.1371/journal.pone.0000207>.
- [22] Guillaume Bastille-Rousseau, Charles B. Yackulic, James Gibbs, Jacqueline L. Frair, Freddy Cabrera, and Stephen Blake. Data from: Migration triggers in a large herbivore: Galápagos giant tortoises navigating resource gradients on volcanoes, 2019. URL <https://www.doi.org/10.5441/001/1.6gr485fk>.
- [23] Guillaume Bastille-Rousseau, Charles B. Yackulic, Jacqueline L. Frair, Freddy Cabrera, and Stephen Blake. Data from: Allometric and temporal scaling of movement characteristics in Galapagos tortoises, 2016. URL <https://doi.org/10.5441/001/1.2cp86266>.
- [24] Guillaume Bastille-Rousseau, Jonathan R. Potts, Charles B. Yackulic, Jacqueline L. Frair, E. Hance Ellington, and Stephen Blake. Data from: Flexible characterization of animal movement pattern using net squared displacement and a latent state model, 2016. URL <https://doi.org/10.5441/001/1.356nb5mf>.
- [25] Guillaume Bastille-Rousseau, Charles B. Yackulic, James P. Gibbs, Jacqueline L. Frair, Freddy Cabrera, and Stephen Blake. Migration triggers in a large herbivore: Galápagos giant tortoises navigating resource gradients on volcanoes. *Ecology*, 100(6):e02658, apr 2019. doi: 10.1002/ecy.2658. URL <https://doi.org/10.1002/ecy.2658>.

- [26] Guillaume Bastille-Rousseau, James P. Gibbs, Charles B. Yackulic, Jacqueline L. Frair, Fredy Cabrera, Louis-Philippe Rousseau, Martin Wikelski, Franz Kümme, and Stephen Blake. Animal movement in the absence of predation: environmental drivers of movement strategies in a partial migration system. *Oikos*, 126(7):1004–1019, jan 2017. doi: 10.1111/oik.03928. URL <https://doi.org/10.1111/oik.03928>.
- [27] Guillaume Bastille-Rousseau, Jonathan R. Potts, Charles B. Yackulic, Jacqueline L. Frair, E. Hance Ellington, and Stephen Blake. Flexible characterization of animal movement pattern using net squared displacement and a latent state model. *Movement Ecology*, 4(1), jun 2016. doi: 10.1186/s40462-016-0080-y. URL <https://doi.org/10.1186/s40462-016-0080-y>.
- [28] Guillaume Bastille-Rousseau, Charles B. Yackulic, Jacqueline L. Frair, Freddy Cabrera, and Stephen Blake. Allometric and temporal scaling of movement characteristics in Galapagos tortoises. *Journal of Animal Ecology*, 85(5):1171–1181, jul 2016. doi: 10.1111/1365-2656.12561. URL <https://doi.org/10.1111/1365-2656.12561>.
- [29] Martin Wikelski, Elena Arriero, Anna Gagliardo, Richard Holland, Markku J. Huttunen, Risto Juvaste, Inge Mueller, Grigori Tertitski, Kasper Thorup, Martin Wild, Markku Alanko, Franz Bairlein, Alexander Cherenkov, Alison Cameron, Reinhard Flatz, Juhani Hannila, Ommo Hüppop, Markku Kangasniemi, Bart Kranstauber, Maija-Liisa Penttinen, Kamran Safi, Vladimir Semashko, Heidi Schmid, and Ralf Wistbacka. Data from: True navigation in migrating gulls requires intact olfactory nerves, 2015. URL <https://doi.org/10.5441/001/1.q986rc29>.
- [30] Martin Wikelski, Elena Arriero, Anna Gagliardo, Richard A. Holland, Markku J. Huttunen, Risto Juvaste, Inge Mueller, Grigori Tertitski, Kasper Thorup, Martin Wild, Markku Alanko, Franz Bairlein, Alexander Cherenkov, Alison Cameron, Reinhard Flatz, Juhani Hannila, Ommo Hüppop, Markku Kangasniemi, Bart Kranstauber, Maija-Liisa Penttinen, Kamran Safi, Vladimir Semashko, Heidi Schmid, and Ralf Wistbacka. True navigation in migrating gulls requires intact olfactory nerves. *Scientific Reports*, 5(1), nov 2015. doi: 10.1038/srep17061. URL <https://doi.org/10.1038/srep17061>.
- [31] Andrea Kölzsch, Erik Kleyheeg, Helmut Kruckenberg, Michael Kaatz, and Bernd Blasius. A periodic Markov model to formalize animal migration on a network. *Royal Society Open Science*, 5(6):180438, jun 2018. doi: 10.1098/rsos.180438. URL <https://doi.org/10.1098/rsos.180438>.
- [32] Evan R. Buechley and Çağan H. Şekercioğlu. Data from: Satellite tracking a wide-ranging endangered vulture species to target conservation actions in the Middle East and East Africa, 2019. URL <https://www.doi.org/10.5441/001/1.385gk270>.
- [33] W. Louis Phipps, Pascual López-López, Evan R. Buechley, Steffen Opiel, Ernesto Álvarez, Volen Arkumarev, Rinur Bekmansurov, Oded Berger-Tal, Ana Bermejo, Anastasios Bounas, Isidoro Carbonell Alanís, Javier

- de la Puente, Vladimir Dobrev, Olivier Duriez, Ron Efrat, Guillaume Fréchet, Javier García, Manuel Galán, Clara García-Ripollés, Alberto Gil, Juan José Iglesias-Lebrija, José Jambas, Igor V. Karyakin, Er-ick Kobierzycki, Elzbieta Kret, Franziska Loercher, Antonio Monteiro, Jon Morant Etxebarria, Stoyan C. Nikolov, José Pereira, Lubomír Peške, Cecile Ponchon, Eduardo Realinho, Victoria Saravia, Çağan H. Şekerciöglü, Theodora Skartsi, José Tavares, Joaquim Teodósio, Vicente Urios, and Núria Vallverdú. Spatial and Temporal Variability in Migration of a Soaring Raptor Across Three Continents. *Frontiers in Ecology and Evolution*, 7, sep 2019. doi: 10.3389/fevo.2019.00323. URL <https://doi.org/10.3389/fevo.2019.00323>.
- [34] Evan R. Buechley, Michael J. McGrady, Emrah Çoban, and Çağan H. Şekerciöglü. Satellite tracking a wide-ranging endangered vulture species to target conservation actions in the Middle East and East Africa. *Biodiversity and Conservation*, 27(9):2293–2310, mar 2018. doi: 10.1007/s10531-018-1538-6. URL <https://doi.org/10.1007/s10531-018-1538-6>.
- [35] Evan R. Buechley, Steffen Opper, William S. Beatty, Stoyan C. Nikolov, Vladimir Dobrev, Volen Arkumarev, Victoria Saravia, Clementine Bougain, Anastasios Bounas, Elzbieta Kret, Theodora Skartsi, Lale Aktay, Karen Aghababayan, Ethan Frehner, and Çağan H. Şekerciöglü. Identifying critical migratory bottlenecks and high-use areas for an endangered migratory soaring bird across three continents. *Journal of Avian Biology*, 49(7):e01629, jul 2018. doi: 10.1111/jav.01629. URL <https://doi.org/10.1111/jav.01629>.
- [36] Andrea Flack, Wolfgang Fiedler, Julio Blas, Ivan Pokrovski, B. Mitropolsky, Michael Kaatz, Karen Aghababayan, A. Khachatryan, Ioannis Fakriadis, Eleni Makrigianni, Leszek Jerzak, M. Shamin, C. Shamina, H. Azafzaf, Claudia Feltrup-Azafzaf, Thabiso M. Mokotjomela, and Martin Wikelski. Data from: Costs of migratory decisions: a comparison across eight white stork populations, 2015. URL <https://www.doi.org/10.5441/001/1.78152p3q>.
- [37] Andrea Flack, Wolfgang Fiedler, Julio Blas, Ivan Pokrovsky, Michael Kaatz, Maxim Mitropolsky, Karen Aghababayan, Ioannis Fakriadis, Eleni Makrigianni, Leszek Jerzak, Hichem Azafzaf, Claudia Feltrup-Azafzaf, Shay Rotics, Thabiso M. Mokotjomela, Ran Nathan, and Martin Wikelski. Costs of migratory decisions: A comparison across eight white stork populations. *Science Advances*, 2(1), jan 2016. doi: 10.1126/sciadv.1500931. URL <https://doi.org/10.1126/sciadv.1500931>.
- [38] Roland Kays, Sarah C. Davidson, Matthias Berger, Gil Bohrer, Wolfgang Fiedler, Andrea Flack, Julian Hirt, Clemens Hahn, Dominik Gauggel, Benedict Russell, Andrea Kölzsch, Ashley Lohr, Jesko Partecke, Michael Quetting, Kamran Safi, Anne Scharf, Gabriel Schneider, Ilona Lang, Friedrich Schaeuffelhut, Matthias Landwehr, Martin Storhas, Louis van Schalkwyk, Candace Vinciguerra, Rolf Weinzierl, and Martin Wikelski. The Movebank system for studying global animal movement and demography. *Methods in Ecology and Evolution*, 13(2):419–431, dec 2021. doi:

10.1111/2041-210x.13767. URL <https://doi.org/10.1111/2041-210x.13767>.

- [39] Keith Bildstein, David Barber, and Marc J. Bechard. Data from: Environmental drivers of variability in the movement ecology of turkey vultures (*Cathartes aura*) in North and South America, 2014. URL <https://doi.org/10.5441/001/1.46ft1k05>.
- [40] Ronaldo Gonçalves Morato, Daniel Luiz Zanella Kantek, Samiko Miyazaki, Thadeu Deluque, and Rogerio Cunha De Paula. Data from: Jaguar movement database—a GPS-based movement dataset of an apex predator in the Neotropics, 2021. URL <https://www.doi.org/10.5441/001/1.3c4fv0m4>.
- [41] Ronaldo G. Morato, Jeffrey J. Thompson, Agustin Paviolo, Jesus A. de La Torre, Fernando Lima, Roy T. McBride, Rogerio C. Paula, Laury Cullen, Leandro Silveira, Daniel L. Z. Kantek, Emiliano E. Ramalho, Louise Maranhão, Mario Haberfeld, Denis A. Sana, Rodrigo A. Medellin, Eduardo Carrillo, Victor Montalvo, Octavio Monroy-Vilchis, Paula Cruz, Anah T. Jacomo, Natalia M. Torres, Giselle B. Alves, Ivonne Cassaigne, Ron Thompson, Carolina Saens-Bolanos, Juan Carlos Cruz, Luiz D. Alfaro, Isabel Hagnauer, Xavier Marina da Silva, Alexandre Vogliotti, Marcela F. D. Moraes, Selma S. Miyazaki, Thadeu D. C. Pereira, Gediendson R. Araujo, Leanes Cruz da Silva, Lucas Leuzinger, Marina M. Carvalho, Lilian Rampin, Leonardo Sartorello, Howard Quigley, Fernando Tortato, Rafael Hoogesteijn, Peter G. Crawshaw, Allison L. Devlin, Joares A. May, Fernando C. C. de Azevedo, Henrique V. B. Concone, Veronica A. Quiroga, Sebastian A. Costa, Juan P. Arrabal, Ezequiel Vanderhoeven, Yamil E. Di Blanco, Alexandre M. C. Lopes, Cynthia E. Widmer, and Milton Cezar Ribeiro. Jaguar movement database: a GPS-based movement dataset of an apex predator in the neotropics. *Ecology*, 99(7):1691–1691, jul 2018. doi: 10.1002/ecy.2379. URL <https://doi.org/10.1002/ecy.2379>.
- [42] R.G. Morato, G.M. Connette, J.A. Stabach, R.C. De Paula, K.M.P.M. Ferraz, D.L.Z. Kantek, S.S. Miyazaki, T.D.C. Pereira, L.C. Silva, A. Paviolo, C. De Angelo, M.S. Di Bitetti, P. Cruz, F. Lima, L. Cullen, D.A. Sana, E.E. Ramalho, M.M. Carvalho, M.X. da Silva, M.D.F. Moraes, A. Vogliotti, J.A. May, M. Haberfeld, L. Rampin, L. Sartorello, G.R. Araujo, G. Wittemyer, M.C. Ribeiro, and P. Leimgruber. Resource selection in an apex predator and variation in response to local landscape characteristics. *Biological Conservation*, 228:233–240, dec 2018. doi: 10.1016/j.biocon.2018.10.022. URL <https://doi.org/10.1016/j.biocon.2018.10.022>.
- [43] Ronaldo G. Morato, Jared A. Stabach, Chris H. Fleming, Justin M. Calabrese, Rogério C. De Paula, Kátia M. P. M. Ferraz, Daniel L. Z. Kantek, Selma S. Miyazaki, Thadeu D. C. Pereira, Gediendson R. Araujo, Agustin Paviolo, Carlos De Angelo, Mario S. Di Bitetti, Paula Cruz, Fernando Lima, Laury Cullen, Denis A. Sana, Emiliano E. Ramalho, Marina M. Carvalho, Fábio H. S. Soares, Barbara Zimbres, Marina X. Silva, Marcela D. F. Moraes, Alexandre Vogliotti, Joares A. May, Mario

- Haberfeld, Lilian Rampim, Leonardo Sartorello, Milton C. Ribeiro, and Peter Leimgruber. Space Use and Movement of a Neotropical Top Predator: The Endangered Jaguar. *PLOS ONE*, 11(12):e0168176, dec 2016. doi: 10.1371/journal.pone.0168176. URL <https://doi.org/10.1371/journal.pone.0168176>.
- [44] Ronaldo G. Morato, Jeffrey J. Thompson, Agustín Paviolo, J. Antonio De La Torre, Fernando Lima, McBride Jr., Roy T., Rogério C. Paula, Cullen Jr., Laury, Leandro Silveira, Daniel L.Z. Kantek, Emiliano E. Ramalho, Louise Maranhão, Mario Haberfeld, Denis A. Sana, Rodrigo A. Medellín, Eduardo Carrillo, Victor Montalvo, Octavio Monroy-Vilchis, Paula Cruz, Anah Tereza Jácomo, Natalia M. Torres, Giselle B. Alves, Ivonne Cassaigne, Ron Thompson, Carolina Saenz-Bolanos, Juan Carlos Cruz, Luis D. Alfaro, Isabel Hagnauer, Marina Xavier Da Silva, Alexandre Vogliotti, Marcela Figuerêdo Duarte Moraes, Selma S. Miyazaki, Thadeu D.C. Pereira, Gediendson R. Araujo, Leanes Cruz Da Silva, Lukas Leuzinger, Marina M Carvalho, Lilian Rampim, Leonardo Sartorello, Howard Quigley, Fernando Tortato, Rafael Hoogesteijn, Crawshaw Jr., Peter G., Allison L. Devlin, May Jr., Joares A., Fernando C.C. De Azevedo, Henrique Villas Boas Concione, Veronica A. Quiroga, Sebastián A. Costa, Juan P. Arrabal, Ezequiel Vanderhoeven, Yamil E. Di Blanco, Alexandre M.C. Lopes, Cynthia E. Widmer, Milton Cezar Ribeiro, Carolina Saens-Bolanos, Luiz D. Alfaro, and Joares A. May. Data from: Jaguar Movement Database: a GPS-based movement dataset of an apex predator in the Neotropics, 2019. URL <https://doi.org/10.5061/dryad.2dh0223>.
- [45] Miltinhoastronauta. Leeclab/Jaguar_Movement: Jaguar Movement Database V1.0 Released!, 2018. URL <https://doi.org/10.5281/zenodo.1345119>.
- [46] Sherub Sherub and Martin Wikelski. Data from: Longer days enable higher diurnal activity for migratory birds [Himalayan griffons], 2021. URL <https://www.doi.org/10.5441/001/1.4n2501f5>.
- [47] Sherub Sherub, Martin Wikelski, Wolfgang Fiedler, and Sarah C. Davidson. Data from: Behavioural adaptations to flight into thin air, 2016. URL <https://doi.org/10.5441/001/1.143v2p2k>.
- [48] Ivan Pokrovsky, Andrea Kölzsch, Sherub Sherub, Wolfgang Fiedler, Peter Glazov, Olga Kulikova, Martin Wikelski, and Andrea Flack. Longer days enable higher diurnal activity for migratory birds. *Journal of Animal Ecology*, 90(9):2161–2171, mar 2021. doi: 10.1111/1365-2656.13484. URL <https://doi.org/10.1111/1365-2656.13484>.
- [49] Sherub Sherub, Gil Bohrer, Martin Wikelski, and Rolf Weinzierl. Behavioural adaptations to flight into thin air. *Biology Letters*, 12(10):20160432, oct 2016. doi: 10.1098/rsbl.2016.0432. URL <https://doi.org/10.1098/rsbl.2016.0432>.
- [50] Yachang Cheng, Wolfgang Fiedler, Martin Wikelski, and Andrea Flack. “closer-to-home” strategy benefits juvenile survival in a long-distance mi-

- gratory bird. *Ecology and Evolution*, 9(16):8945–8952, jul 2019. doi: 10.1002/ece3.5395. URL <https://doi.org/10.1002/ece3.5395>.
- [51] Rolf Weinzierl, Gil Bohrer, Bart Kranstauber, Wolfgang Fiedler, Martin Wikelski, and Andrea Flack. Wind estimation based on thermal soaring of birds. *Ecology and Evolution*, 6(24):8706–8718, nov 2016. doi: 10.1002/ece3.2585. URL <https://doi.org/10.1002/ece3.2585>.
- [52] Wolfgang Fiedler, Elke Leppelsack, Hans Leppelsack, Thomas Stahl, Oda Wieding, and Martin Wikelski. Data from: Study "LifeTrack White Stork Bavaria" (2014-2019), 2019. URL <https://www.doi.org/10.5441/001/1.v1cs4nn0>.
- [53] Roland Kays, Margaret C. Crofoot, Walter Jetz, and Martin Wikelski. Terrestrial animal tracking as an eye on life and planet. *Science*, 348(6240), jun 2015. doi: 10.1126/science.aaa2478. URL <https://doi.org/10.1126/science.aaa2478>.
- [54] Andrea Kölzsch, Helmut Kruckenberg, Peter Glazov, Gerhard J.D.M. Müskens, and Martin Wikelski. Data from: Towards a new understanding of migration timing: slower spring than autumn migration in geese reflects different decision rules for stopover use and departure, 2016. URL <https://www.doi.org/10.5441/001/1.31c2v92f>.
- [55] Andrea Kölzsch, Gerhard J. D. M. Müskens, Helmut Kruckenberg, Peter Glazov, Rolf Weinzierl, Bart A. Nolet, and Martin Wikelski. Towards a new understanding of migration timing: slower spring than autumn migration in geese reflects different decision rules for stopover use and departure. *Oikos*, 125(10):1496–1507, feb 2016. doi: 10.1111/oik.03121. URL <https://doi.org/10.1111/oik.03121>.
- [56] Wolfgang Fiedler, Walter Niederer, Alwin Schönenberger, Andrea Flack, and Martin Wikelski. Data from: Study "LifeTrack White Stork Vorarlberg" (2016-2019), 2019. URL <https://www.doi.org/10.5441/001/1.71r7pp6q>.
- [57] A. David M. Latham and Stan Boutin. Data from: Wolf ecology and caribou-primary prey-wolf spatial relationships in low productivity peatland complexes in northeastern Alberta, 2019. URL <https://www.doi.org/10.5441/001/1.7vr1k987>.
- [58] A. David M. Latham, M. Cecilia Latham, Mark S. Boyce, and Stan Boutin. Movement responses by wolves to industrial linear features and their effect on woodland caribou in northeastern Alberta. *Ecological Applications*, 21(8):2854–2865, dec 2011. doi: 10.1890/11-0666.1. URL <https://doi.org/10.1890/11-0666.1>.
- [59] Wibke Peters, Mark Hebblewhite, Nicholas DeCesare, Francesca Cagnacci, and Marco Musiani. Resource separation analysis with moose indicates threats to caribou in human altered landscapes. *Ecography*, 36(4):487–498, oct 2012. doi: 10.1111/j.1600-0587.2012.07733.x. URL <https://doi.org/10.1111/j.1600-0587.2012.07733.x>.

- [60] Jared A. Stabach, Lacey F. Hughey, Robin S. Reid, Jeffrey S. Worden, Peter Leimgruber, and Randall B. Boone. Data from: Study "White-bearded wildebeest in Kenya", 2020. URL <https://www.doi.org/10.5441/001/1.h0t27719>.
- [61] Mark Hebblewhite and Evelyn Merrill. Modelling wildlife-human relationships for social species with mixed-effects resource selection models. *Journal of Applied Ecology*, 45(3):834–844, jul 2007. doi: 10.1111/j.1365-2664.2008.01466.x. URL <https://doi.org/10.1111/j.1365-2664.2008.01466.x>.
- [62] Mark Hebblewhite and Evelyn H. Merrill. Multiscale wolf predation risk for elk: does migration reduce risk? *Oecologia*, 152(2):377–387, feb 2007. doi: 10.1007/s00442-007-0661-y. URL <https://doi.org/10.1007/s00442-007-0661-y>.
- [63] Wolfgang Fiedler, Andrea Flack, Andreas Schmidt, Ute Reinhard, and Martin Wikelski. Data from: Study "LifeTrack White Stork Oberschwaben" (2014-2019), 2019. URL <https://www.doi.org/10.5441/001/1.c42j3js7>.
- [64] Keith L. Bildstein, David Barber, Marc J. Bechard, and Maricel Graña Grilli. Data from: Wing size but not wing shape is related to migratory behavior in a soaring bird, 2016. URL <https://www.doi.org/10.5441/001/1.37r2b884>.
- [65] Shay Rotics, Michael Kaatz, Sondra Turjeman, Damaris Zurell, Martin Wikelski, Nir Sapir, Ute Eggers, Wolfgang Fiedler, Florian Jeltsch, and Ran Nathan. Data from: Early arrival at breeding grounds: causes, costs and a trade-off with overwintering latitude, 2018. URL <https://www.doi.org/10.5441/001/1.v8d24552>.
- [66] Shay Rotics, Michael Kaatz, Sondra Turjeman, Damaris Zurell, Martin Wikelski, Nir Sapir, Ute Eggers, Wolfgang Fiedler, Florian Jeltsch, and Ran Nathan. Early arrival at breeding grounds: Causes, costs and a trade-off with overwintering latitude. *Journal of Animal Ecology*, 87(6): 1627–1638, oct 2018. doi: 10.1111/1365-2656.12898. URL <https://doi.org/10.1111/1365-2656.12898>.
- [67] Anny Anselin, Peter Desmet, Tanja Milotic, Kjell Janssens, Filiep T'Jollyn, Luc De Bruyn, and Willem Bouten. MH_WATERLAND - Western marsh harriers (*Circus aeruginosus*, Accipitridae) breeding near the Belgium-Netherlands border, 2022. URL <https://doi.org/10.5281/zenodo.3532940>.
- [68] Andrea Kölzsch, Gerhard J.D.M. Müskens, Sander Moonen, Helmut Kruckenberg, Peter Glazov, and Martin Wikelski. Data from: Flyway connectivity and exchange primarily driven by moult migration in geese [North Sea population], 2019. URL <https://www.doi.org/10.5441/001/1.ct72m82n>.
- [69] A. Kölzsch, G. J. D. M. Müskens, P. Szinai, S. Moonen, P. Glazov, H. Kruckenberg, M. Wikelski, and B. A. Nolet. Flyway connectivity

- and exchange primarily driven by moult migration in geese. *Movement Ecology*, 7(1), jan 2019. doi: 10.1186/s40462-019-0148-6. URL <https://doi.org/10.1186/s40462-019-0148-6>.
- [70] Gerhard J.D.M. Müskens, Péter Szinai, Tamas Sapi, Andrea Kölzsch, Martin Wikelski, and Bart A. Nolet. Data from: Flyway connectivity and exchange primarily driven by moult migration in geese [Pannonic population], 2019. URL <https://www.doi.org/10.5441/001/1.46b0mq21>.
- [71] Rob Slotow, Maria Thaker, and Abi Tamim Vanak. Data from: Fine-scale tracking of ambient temperature and movement reveals shuttling behavior of elephants to water, 2019. URL <https://www.doi.org/10.5441/001/1.403h24q5>.
- [72] Maria Thaker, Pratik R. Gupte, Herbert H. T. Prins, Rob Slotow, and Abi T. Vanak. Fine-Scale Tracking of Ambient Temperature and Movement Reveals Shuttling Behavior of Elephants to Water. *Frontiers in Ecology and Evolution*, 7, jan 2019. doi: 10.3389/fevo.2019.00004. URL <https://doi.org/10.3389/fevo.2019.00004>.
- [73] Mark Hebblewhite, Evelyn H. Merrill, Hans Martin, Jodi E. Berg, Holger Bohm, and Scott L. Eggeman. Data from: Study "Ya Ha Tinda elk project, Banff National Park, 2001-2020 (females)", 2020. URL <https://www.doi.org/10.5441/001/1.5g4h5t6c>.
- [74] Marlee A. Tucker, Katrin Böhning-Gaese, William F. Fagan, John M. Fryxell, Bram Van Moorter, Susan C. Alberts, Abdullahi H. Ali, Andrew M. Allen, Nina Attias, Tal Avgar, Hattie Bartlam-Brooks, Buuveibaatar Bayarbaatar, Jerrold L. Belant, Alessandra Bertassoni, Dean Beyer, Laura Bidner, Floris M. van Beest, Stephen Blake, Niels Blaum, Chloe Bracis, Danielle Brown, P. J. Nico de Bruyn, Francesca Cagnacci, Justin M. Calabrese, Constança Camilo-Alves, Simon Chamaillé-Jammes, Andre Chiaradia, Sarah C. Davidson, Todd Dennis, Stephen DeStefano, Duane Diefenbach, Iain Douglas-Hamilton, Julian Fennessy, Claudia Fichtel, Wolfgang Fiedler, Christina Fischer, Ilya Fischhoff, Christen H. Fleming, Adam T. Ford, Susanne A. Fritz, Benedikt Gehr, Jacob R. Goheen, Eliezer Gurarie, Mark Hebblewhite, Marco Heurich, A. J. Mark Hewison, Christian Hof, Edward Hurme, Lynne A. Isbell, René Janssen, Florian Jeltsch, Petra Kaczensky, Adam Kane, Peter M. Kappeler, Matthew Kauffman, Roland Kays, Duncan Kimuyu, Flavia Koch, Bart Kranstauber, Scott LaPoint, Peter Leimgruber, John D. C. Linnell, Pascual López-López, A. Catherine Markham, Jenny Mattisson, Emilia Patricia Medici, Ugo Mellone, Evelyn Merrill, Guilherme de Miranda Mourão, Ronaldo G. Morato, Nicolas Morellet, Thomas A. Morrison, Samuel L. Díaz-Muñoz, Atle Mysterud, Dejid Nandintsetseg, Ran Nathan, Aidin Niamir, John Odden, Robert B. O'Hara, Luiz Gustavo R. Oliveira-Santos, Kirk A. Olson, Bruce D. Patterson, Rogerio Cunha de Paula, Luca Pedrotti, Björn Reineking, Martin Rimpler, Tracey L. Rogers, Christer Moe Rolandsen, Christopher S. Rosenberry, Daniel I. Rubenstein, Kamran Safi, Sonia Said, Nir Sapir, Hall Sawyer, Niels Martin Schmidt, Nuria Selva, Agnieszka Sergiel, Enkhtuvshin Shiilegdamba, João Paulo Silva, Navinder Singh, Erling J. Solberg, Orr Spiegel, Olav Strand, Siva Sundaresan,

- Wiebke Ullmann, Ulrich Voigt, Jake Wall, David Wattles, Martin Wikel-ski, Christopher C. Wilmers, John W. Wilson, George Wittemyer, Filip Zięba, Tomasz Zwijacz-Kozica, and Thomas Mueller. Moving in the An-thropocene: Global reductions in terrestrial mammalian movements. *Sci-ence*, 359(6374):466–469, jan 2018. doi: 10.1126/science.aam9712. URL <https://www.doi.org/10.1126/science.aam9712>.
- [75] Scott L. Eggeman, Mark Hebblewhite, Holger Bohm, Jesse Whittington, and Evelyn H. Merrill. Behavioural flexibility in migratory behaviour in a long-lived large herbivore. *Journal of Animal Ecology*, 85(3):785–797, mar 2016. doi: 10.1111/1365-2656.12495. URL <https://www.doi.org/10.1111/1365-2656.12495>.
- [76] MARK HEBBLEWHITE, EVELYN H. MERRILL, LUIGI E. MORGAN-TINI, CLIFFORD A. WHITE, JAMES R. ALLEN, ELDON BRUNS, LINDA THURSTON, and TOMAS E. HURD. Is the migratory be-havior of montane elk herds in peril? the case of alberta's ya ha tinda elk herd. *Wildlife Society Bulletin*, 34(5):1280–1294, dec 2006. doi: 10.2193/0091-7648(2006)34[1280:itmbom]2.0.co;2. URL [https://www.doi.org/10.2193/0091-7648\(2006\)34\[1280:ITMBOM\]2.0.CO;2](https://www.doi.org/10.2193/0091-7648(2006)34[1280:ITMBOM]2.0.CO;2).
- [77] Mark Hebblewhite and Evelyn H. Merrill. Trade-offs between predation risk and forage differ between migrant strategies in a migratory ungu-late. *Ecology*, 90(12):3445–3454, dec 2009. doi: 10.1890/08-2090.1. URL <https://www.doi.org/10.1890/08-2090.1>.
- [78] Mark Hebblewhite, Evelyn Merrill, and Greg McDermid. A MULTI-SCALE TEST OF THE FORAGE MATURATION HYPOTHESIS IN a PARTIALLY MIGRATORY UNGULATE POPULATION. *Ecological Monographs*, 78(2):141–166, may 2008. doi: 10.1890/06-1708.1. URL <https://www.doi.org/10.1890/06-1708.1>.
- [79] Ben Koks, Almut Schlaich, Tonio Schaub, Raymond Klaassen, Anny Anselin, Peter Desmet, Tanja Milotic, Kjell Janssens, and Willem Bouten. H_GRONINGEN - Western marsh harriers (*Circus aeruginosus*, Accip-itridae) breeding in Groningen (the Netherlands), 2022. URL <https://doi.org/10.5281/zenodo.3552507>.
- [80] Mark S. Boyce and Simone Ciuti. Data from: Human selection of elk behavioural traits in a landscape of fear, 2020. URL <https://www.doi.org/10.5441/001/1.j484vk24>.
- [81] Dale G. Paton, Simone Ciuti, Michael Quinn, and Mark S. Boyce. Hunting exacerbates the response to human disturbance in large herbivores while migrating through a road network. *Ecosphere*, 8(6), jun 2017. doi: 10.1002/ecs2.1841. URL <https://doi.org/10.1002/ecs2.1841>.
- [82] Christina M. Prokopenko, Mark S. Boyce, and Tal Avgar. Characterizing wildlife behavioural responses to roads using integrated step selection analysis. *Journal of Applied Ecology*, 54(2):470–479, sep 2016. doi: 10.1111/1365-2664.12768. URL <https://doi.org/10.1111/1365-2664.12768>.

- [83] Christina M. Prokopenko, Mark S. Boyce, and Tal Avgar. Extent-dependent habitat selection in a migratory large herbivore: road avoidance across scales. *Landscape Ecology*, 32(2):313–325, oct 2016. doi: 10.1007/s10980-016-0451-1. URL <https://doi.org/10.1007/s10980-016-0451-1>.
- [84] David R. Roberts, Volker Bahn, Simone Ciuti, Mark S. Boyce, Jane Elith, Gurutzeta Guillera-Arroita, Severin Hauenstein, José J. Lahoz-Monfort, Boris Schröder, Wilfried Thuiller, David I. Warton, Brendan A. Wintle, Florian Hartig, and Carsten F. Dormann. Cross-validation strategies for data with temporal, spatial, hierarchical, or phylogenetic structure. *Ecography*, 40(8):913–929, mar 2017. doi: 10.1111/ecog.02881. URL <https://doi.org/10.1111/ecog.02881>.
- [85] Henrik Thurfjell, Simone Ciuti, and Mark S. Boyce. Learning from the mistakes of others: How female elk (*Cervus elaphus*) adjust behaviour with age to avoid hunters. *PLOS ONE*, 12(6):e0178082, jun 2017. doi: 10.1371/journal.pone.0178082. URL <https://doi.org/10.1371/journal.pone.0178082>.
- [86] Robin A. Benz, Mark S. Boyce, Henrik Thurfjell, Dale G. Paton, Marco Musiani, Carsten F. Dormann, and Simone Ciuti. Dispersal Ecology Informs Design of Large-Scale Wildlife Corridors. *PLOS ONE*, 11(9):e0162989, sep 2016. doi: 10.1371/journal.pone.0162989. URL <https://doi.org/10.1371/journal.pone.0162989>.
- [87] Erik P. Ensing, Simone Ciuti, Freek A. L. M. de Wijs, Dennis H. Lentferink, André ten Hoedt, Mark S. Boyce, and Roelof A. Hut. GPS based daily activity patterns in european red deer and north american elk (*cervus elaphus*): Indication for a weak circadian clock in ungulates. *PLoS ONE*, 9(9):e106997, sep 2014. doi: 10.1371/journal.pone.0106997. URL <https://doi.org/10.1371/journal.pone.0106997>.
- [88] Joshua Killeen, Henrik Thurfjell, Simone Ciuti, Dale Paton, Marco Musiani, and Mark S Boyce. Habitat selection during ungulate dispersal and exploratory movement at broad and fine scale with implications for conservation management. *Movement Ecology*, 2(1), jul 2014. doi: 10.1186/s40462-014-0015-4. URL <https://doi.org/10.1186/s40462-014-0015-4>.
- [89] Henrik Thurfjell, Simone Ciuti, and Mark S Boyce. Applications of step-selection functions in ecology and conservation. *Movement Ecology*, 2(1), feb 2014. doi: 10.1186/2051-3933-2-4. URL <https://doi.org/10.1186/2051-3933-2-4>.
- [90] Simone Ciuti, Tyler B. Muhly, Dale G. Paton, Allan D. McDevitt, Marco Musiani, and Mark S. Boyce. Human selection of elk behavioural traits in a landscape of fear. *Proceedings of the Royal Society B: Biological Sciences*, 279(1746):4407–4416, sep 2012. doi: 10.1098/rspb.2012.1483. URL <https://doi.org/10.1098/rspb.2012.1483>.

- [91] Simone Ciuti, Joseph M. Northrup, Tyler B. Muhly, Silvia Simi, Marco Musiani, Justin A. Pitt, and Mark S. Boyce. Effects of Humans on Behaviour of Wildlife Exceed Those of Natural Predators in a Landscape of Fear. *PLoS ONE*, 7(11):e50611, nov 2012. doi: 10.1371/journal.pone.0050611. URL <https://doi.org/10.1371/journal.pone.0050611>.
- [92] Geert Spanoghe, Peter Desmet, Tanja Milotic, Kjell Janssens, Nico De Regge, Joost Vanoverbeke, and Willem Bouten. MH_ANTWERPEN - Western marsh harriers (*Circus aeruginosus*, Accipitridae) breeding near Antwerp (Belgium), 2022. URL <https://doi.org/10.5281/zenodo.3550093>.
- [93] Eric W.M. Stienen, Peter Desmet, Tanja Milotic, Francisco Hernandez, Klaas Deneudt, Willem Bouten, Wendt Müller, Hans Matheve, and Luc Lens. LBBG_ZEEBRUGGE - Lesser black-backed gulls (*Larus fuscus*, Laridae) breeding at the southern North Sea coast (Belgium and the Netherlands), 2022. URL <https://doi.org/10.5281/zenodo.3540799>.
- [94] Eric W.M. Stienen, Peter Desmet, Tanja Milotic, Francisco Hernandez, Klaas Deneudt, Hans Matheve, and Willem Bouten. HG_OOSTENDE - Herring gulls (*Larus argentatus*, Laridae) breeding at the southern North Sea coast (Belgium), 2022. URL <https://doi.org/10.5281/zenodo.3541811>.
- [95] Rascha J.M. Nuijten, Theo Gerrits, Peter P. De Vries, Gerhard J.D.M. Müskens, and Bart A. Nolet. Data from: Less is more: on-board lossy compression of accelerometer data increases biologging capacity, 2020. URL <https://www.doi.org/10.5441/001/1.8ms7mm80>.
- [96] Rascha J. M. Nuijten, Theo Gerrits, Judy Shamoun-Baranes, and Bart A. Nolet. Less is more: On-board lossy compression of accelerometer data increases biologging capacity. *Journal of Animal Ecology*, 89(1):237–247, jan 2020. doi: 10.1111/1365-2656.13164. URL <https://www.doi.org/10.1111/1365-2656.13164>.
- [97] Andrea Kölzsch, Gerhard J.D.M. Müskens, Peter Glazov, Helmut Kruckenberg, and Martin Wikelski. Data from: Goose parents lead migration V, 2020. URL <https://www.doi.org/10.5441/001/1.ms87s2m6>.
- [98] A. Kölzsch, A. Flack, G. J. D. M. Müskens, H. Kruckenberg, P. Glazov, and M. Wikelski. Goose parents lead migration V. *Journal of Avian Biology*, 51(3), mar 2020. doi: 10.1111/jav.02392. URL <https://doi.org/10.1111/jav.02392>.
- [99] Robert A. Ronconi and Katherine R. Shlepr. Data from: Study "Herring Gulls (*Larus Argentatus*); Ronconi; Brier Island, Canada", 2020. URL <https://www.doi.org/10.5441/001/1.282vr7kd>.
- [100] Christine M. Anderson, H. Grant Gilchrist, Robert A. Ronconi, Katherine R. Shlepr, Daniel E. Clark, David A. Fifield, Gregory J. Robertson, and Mark L. Mallory. Both short and long distance migrants use energy-minimizing migration strategies in North American herring gulls. *Movement Ecology*, 8(1), jun 2020. doi: 10.1186/s40462-020-00207-9. URL <https://doi.org/10.1186/s40462-020-00207-9>.

- [101] Daniel E. Clark, Stuart A. Mackenzie, Kiana Koenen, Jillian Whitney, and Stephen DeStefano. Data from: Study "Herring Gulls (*Larus Argentatus*); Clark; Massachussets, United States", 2020. URL <https://www.doi.org/10.5441/001/1.3th8b5q3>.
- [102] Robert A. Ronconi and Philip D. Taylor. Data from: Study "Herring Gulls (*Larus Argentatus*); Ronconi; Sable Island, Canada", 2020. URL <https://www.doi.org/10.5441/001/1.3264ss3v>.
- [103] Katherine Mertes, Walter Jetz, and Martin Wikelski. Data from: Hierarchical multi-grain models improve descriptions of species' environmental associations, distribution, and abundance, 2020. URL <https://www.doi.org/10.5441/001/1.cp97k9j1>.
- [104] Katherine Mertes, Marta A. Jarzyna, and Walter Jetz. Hierarchical multi-grain models improve descriptions of species' environmental associations, distribution, and abundance. *Ecological Applications*, 30(6), may 2020. doi: 10.1002/eap.2117. URL <https://doi.org/10.1002/eap.2117>.
- [105] Andy M Ramey, S.A. Hatch, Christina A Ahlstrom, M.L. Van Toor, H. Woksepp, J.C. Chandler, John A Reed, Andrew Reeves, J. Waldenstrom, A.B. Franklin, J. Bonnedahl, V.A. Gill, D.M. Mulcahy, and David C Douglas. Tracking Data for Three Large-bodied Gull Species and Hybrids (*Larus* spp.), 2020. URL <https://doi.org/10.5066/P9FZ40JW>.
- [106] Geert Spanoghe, Peter Desmet, Tanja Milotic, Gunther Van Ryckegem, Joost Vanoverbeke, Bruno J. Ens, and Willem Bouten. O_WESTERSCHELDE - Eurasian oystercatchers (*Haematopus ostralegus*, *Haematopodidae*) breeding in East Flanders (Belgium), 2022. URL <https://doi.org/10.5281/zenodo.3734898>.
- [107] Eric W.M. Stienen, Wendt Müller, Luc Lens, Tanja Milotic, and Peter Desmet. LBBG_JUVENILE - Juvenile lesser black-backed gulls (*Larus fuscus*, *Laridae*) hatched in Zeebrugge (Belgium), 2022. URL <https://doi.org/10.5281/zenodo.5075868>.
- [108] R. John Power and Stephen Dell. Data from: A note on the reestablishment of the cheetah population in the Pilanesberg National Park, South Africa, 2020. URL <https://doi.org/10.5441/001/1.k6b630mv>.
- [109] R. John Power, Vincent Van der Merwe, Samantha Page-Nicholson, Mia V. Botha, Stephen Dell, and Pieter Nel. A Note on the Reestablishment of the Cheetah Population in the Pilanesberg National Park, South Africa. *African Journal of Wildlife Research*, 49(1), feb 2019. doi: 10.3957/056.049.0012. URL <https://doi.org/10.3957/056.049.0012>.
- [110] Geert Spanoghe, Kjell Janssens, Raymond Klaassen, Tonio Schaub, Tanja Milotic, and Peter Desmet. BOP_RODENT - Rodent specialized birds of prey (*Circus*, *Asio*, *Buteo*) in Flanders (Belgium), 2022. URL <https://doi.org/10.5281/zenodo.5735405>.
- [111] Philipp Schwemmer and Stefan Garthe. Data from: Migrating curlews on schedule: departure and arrival patterns of a long-distance migrant

- depend on time and breeding location rather than on wind conditions, 2021. URL <https://www.doi.org/10.5441/001/1.715k46g2>.
- [112] Philipp Schwemmer, Moritz Mercker, Klaus Heinrich Vanselow, Pier-rick Bocher, and Stefan Garthe. Migrating curlews on schedule: departure and arrival patterns of a long-distance migrant depend on time and breeding location rather than on wind conditions. *Movement Ecology*, 9(1), mar 2021. doi: 10.1186/s40462-021-00252-y. URL <https://doi.org/10.1186/s40462-021-00252-y>.
- [113] Ben Carlson, Shay Rotics, Ran Nathan, Martin Wikelski, and Walter Jetz. Data from: Individual environmental niches in mobile organisms, 2021. URL <https://doi.org/10.5441/001/1.rj21g1p1>.
- [114] Ben S. Carlson, Shay Rotics, Ran Nathan, Martin Wikelski, and Walter Jetz. Individual environmental niches in mobile organisms. *Nature Communications*, 12(1), jul 2021. doi: 10.1038/s41467-021-24826-x. URL <https://doi.org/10.1038/s41467-021-24826-x>.
- [115] Antti Piironen, Antti Paasivaara, and Toni Laaksonen. Data from: Birds of three worlds: moult migration to high Arctic expands a boreal-temperate flyway to a third biome, 2021. URL <https://www.doi.org/10.5441/001/1.22kk5126>.
- [116] Antti Piironen, Antti Paasivaara, and Toni Laaksonen. Birds of three worlds: moult migration to high Arctic expands a boreal-temperate flyway to a third biome. *Movement Ecology*, 9(1), sep 2021. doi: 10.1186/s40462-021-00284-4. URL <https://www.doi.org/10.1186/s40462-021-00284-4>.
- [117] Mathieu Basille, Rena R. Borkhataria, A. Lawrence Bryan, David N. Bucklin, Simona Picardi, and Peter C. Frederick. Data from: Study "Wood stork (*Mycteria americana*) Southeastern US 2004–2019", 2021. URL <https://www.doi.org/10.5441/001/1.r0h6725k>.
- [118] Simona Picardi, Peter C. Frederick, Rena R. Borkhataria, and Mathieu Basille. Partial migration in a subtropical wading bird in the southeastern United States. *Ecosphere*, 11(2), feb 2020. doi: 10.1002/ecs2.3054. URL <https://doi.org/10.1002/ecs2.3054>.
- [119] Adriaan M. Dokter, Kees Oosterbeek, Martin J. Baptist, Peter Desmet, Henk-Jan van der Kolk, Willem Bouten, and Bruno J. Ens. O_BALGZAND - Eurasian oystercatchers (*Haematopus ostralegus*, Haematopodidae) wintering on Balgzand (the Netherlands), 2022. URL <https://doi.org/10.5281/zenodo.5653441>.
- [120] Kees Oosterbeek, Roeland A. Bom, Judy Shamoun-Baranes, Peter Desmet, Henk-Jan van der Kolk, Willem Bouten, and Bruno J. Ens. O_SCHIERMONNIKOOG - Eurasian oystercatchers (*Haematopus ostralegus*, Haematopodidae) breeding on Schiermonnikoog (the Netherlands), 2022. URL <https://doi.org/10.5281/zenodo.5653477>.

- [121] Henk-Jan van der Kolk, Kees Oosterbeek, Eelke Jongejans, Magali Frauendorf, Andrew M. Allen, Willem Bouten, Peter Desmet, Hans de Kroon, Bruno J. Ens, and Martijn van de Pol. O_VLIELAND - Eurasian oystercatchers (*Haematopus ostralegus*, Haematopodidae) breeding and wintering on Vlieland (the Netherlands), 2022. URL <https://doi.org/10.5281/zenodo.5653890>.
- [122] Kees Oosterbeek, Jan de Jong, Peter Desmet, Henk-Jan van der Kolk, Willem Bouten, and Bruno J. Ens. O_AMELAND - Eurasian oystercatchers (*Haematopus ostralegus*, Haematopodidae) breeding on Ameland (the Netherlands), 2022. URL <https://doi.org/10.5281/zenodo.5647596>.
- [123] Graeme C. Hays, Jeanne A. Mortimer, Alex Rattray, Takahiro Shimada, and Nicole Esteban. Data from: High accuracy tracking reveals how small conservation areas can protect marine megafauna, 2021. URL <https://www.doi.org/10.5441/001/1.r72ph75f>.
- [124] Graeme C. Hays, Jeanne A. Mortimer, Alex Rattray, Takahiro Shimada, and Nicole Esteban. High accuracy tracking reveals how small conservation areas can protect marine megafauna. *Ecological Applications*, 31(7), aug 2021. doi: 10.1002/eap.2418. URL <https://www.doi.org/10.1002/eap.2418>.
- [125] Mariëlle L. Van Toor, Sergey Kharitonov, Saulius Švažas, Mindaugas Dagys, Eric Kleyheeg, Gerard Müskens, Ulf Ottosson, Ramunas Žydelis, and Jonas Waldenström. Data from: Study "Eurasian wigeon (*Mareca penelope*) Netherlands Lithuania 2018-2019", 2021. URL <https://www.doi.org/10.5441/001/1.dv5mm289>.
- [126] Mariëlle L. van Toor, Sergey Kharitonov, Saulius Švažas, Mindaugas Dagys, Erik Kleyheeg, Gerard Müskens, Ulf Ottosson, Ramunas Žydelis, and Jonas Waldenström. Migration distance affects how closely Eurasian wigeons follow spring phenology during migration. *Movement Ecology*, 9(1), dec 2021. doi: 10.1186/s40462-021-00296-0. URL <https://doi.org/10.1186/s40462-021-00296-0>.
- [127] Martin Wikelski. MPIAB PNIC hurricane frigate tracking, 2016. Movebank study 6770990 (accessed on 15 February 2022).
- [128] Martin Wikelski, Ran Nathan, and Shay Rotics. HUI MPIAB White Stork GSM E-Obs, 2015. Movebank study 7002955 (accessed on 15 February 2022).
- [129] Stephen Blake, Randy Arndt, and Doug Ladd. Dunn Ranch Bison Tracking Project, 2017. Movebank study 8019591 (accessed on 15 February 2022).
- [130] Roland Kays. LifeTrack - Great Egrets, 2017. Movebank study 8849813 (accessed on 15 February 2022).
- [131] Martin Wikelski, Ran Nathan, and Shay Rotics. HUI MPIAB White Stork E-Obs, 2022. Movebank study 8863543 (accessed on 15 February 2022).

- [132] Martin Wikelski. LifeTrack White Stork Uzbekistan, 2021. Movebank study 9493881 (accessed on 15 February 2022).
- [133] H. Azafzaf, C. Feltrup-Azafzaf, A. Flack, M. Wikelski, and W. Fiedler. LifeTrack White Stork Tunisia, 2015. Movebank study 10157679 (accessed on 15 February 2022).
- [134] Barb Jensen. Pandion haliaetus Osprey - SouthEast Michigan, 2018. Movebank study 10204361 (accessed on 15 February 2022).
- [135] Martin Wikelski. LifeTrack White Stork Loburg, 2022. Movebank study 10449318 (accessed on 15 February 2022).
- [136] Martin Wikelski, Ran Nathan, and Shay Rotics. HUI MPIAB White Stork GSM 2013, 2022. Movebank study 10449698 (accessed on 15 February 2022).
- [137] David Barber. Hooded Vulture Africa, 2022. Movebank study 14671003 (accessed on 15 February 2022).
- [138] Stefan Garthe. FTZ Geese Wadden Sea, 2022. Movebank study 69724677 (accessed on 15 February 2022).
- [139] Dmitrijs Boiko. LifeTrack Whooper Swan Latvia, 2017. Movebank study 92261778 (accessed on 15 February 2022).
- [140] Wolfgang Fiedler. LifeTrack Ducks Lake Constance, 2021. Movebank study 236953686 (accessed on 15 February 2022).
- [141] Ryan Askren. Canada geese (*Branta canadensis*), 2022. Movebank study 329155299 (accessed on 15 February 2022).
- [142] Paweł Mirski. White-tailed Eagle Poland., 2015. Movebank study 384868221 (accessed on 15 February 2022).
- [143] Laurel Serieys. Coyote Valley Bobcat Habitat Connectivity Study, 2018. Movebank study 475878514 (accessed on 15 February 2022).
- [144] Laurel Serieys. Aromas Hills Bobcat Habitat Connectivity Study, 2018. Movebank study 501787846 (accessed on 15 February 2022).
- [145] Harald Grabenhofer. Graugans Zugverhalten Neusiedler See, 2022. Movebank study 505156776 (accessed on 15 February 2022).
- [146] Patrick Scherler. *Milvus_milvus_atlantismarcuard*, 2021. Movebank study 672882373 (accessed on 15 February 2022).
- [147] James P. Lawler. NPS Dall Sheep in Yukon-Charley Rivers National Preserve, 2003. Movebank study 673728219 (accessed on 15 February 2022).
- [148] Perilhon. *Milvus migrans*, 2022. Movebank study 892924356 (accessed on 15 February 2022).
- [149] Thierry Boulinier. ECOPATH, Brown skua, Boulinier et al., Amsterdam Island, 2020. Movebank study 918219824 (accessed on 15 February 2022).

- [150] Frédéric Jiguet. Birdman research project. Tracking curlews to unravel migration connectivity., 2022. Movebank study 1077731101 (accessed on 15 February 2022).
- [151] Scott LaPoint. Carnivore movements near Black Rock Forest New York, 2021. Movebank study 1088836380 (accessed on 15 February 2022).
- [152] Chris H. Fleming. GPS calibration data (global), 2019. Movebank study 1092737859 (accessed on 15 February 2022).
- [153] Morten Frederiksen. Ivory gull N Greenland 2018/19, 2023. Movebank study 1123149708 (accessed on 15 February 2022).
- [154] INTERREX. Caspian Gulls - Poland, 2020. Movebank study 1208105916 (accessed on 15 February 2022).
- [155] Petras Kurlavičius. Common Crane 2020 (Lithuanian University of Educational Studies; LEU), 2022. Movebank study 1229945587 (accessed on 15 February 2022).
- [156] Dominique Berteaux. Arctic fox Bylot - GPS tracking, 2021. Movebank study 1241071371 (accessed on 15 February 2022).
- [157] Frédéric Jiguet. Corvus corone [ID_PROG 883], 2022. Movebank study 1266784970 (accessed on 15 February 2022).
- [158] Jérôme Cavailles. Monitoring of Capra ibex (Bovidae) populations in the western alps (project ALCOTRA LEMED-IBEX), 2020. Movebank study 1285079529 (accessed on 15 February 2022).
- [159] Martin Wikelski. Cathartes aura MPIAB Cuba, 2022. Movebank study 1393954358 (accessed on 15 February 2022).
- [160] Jelle Loonstra. Lapwing NFW Vanellus Vanellus, 2022. Movebank study 1448409403 (accessed on 15 February 2022).
- [161] Sinan Robillard. Variability of White Stork flight patterns prior to earthquakes, 2021. Movebank study 1498452485 (accessed on 15 February 2022).
- [162] Wolfgang Fiedler. LifeTrack White Stork Sarralbe [ID_PROG 1093], 2022. Movebank study 1562253659 (accessed on 15 February 2022).
- [163] Willem Burger. Tchad Redneck Ostrich, 2022. Movebank study 1671751878 (accessed on 15 February 2022).
- [164] Patricia Medici. Lowland tapirs, Tapirus terrestris, in Southern Brazil, 2019. Movebank study 1907973121 (accessed on 15 February 2022).
- [165] Diana Solovyeva. Vega gull (Larus vegae) - GPS - Russia South Korea Japan, 2019. Movebank study 1907974323 (accessed on 15 February 2022).
- [166] Ikuya Yamada, Akari Asai, Jin Sakuma, Hiroyuki Shindo, Hideaki Takeda, Yoshiyasu Takefuji, and Yuji Matsumoto. Wikipedia2Vec: An Efficient Toolkit for Learning and Visualizing the Embeddings of Words

- and Entities from Wikipedia. In *Proceedings of the 2020 Conference on Empirical Methods in Natural Language Processing: System Demonstrations*, pages 23–30, Online, October 2020. Association for Computational Linguistics. doi: 10.18653/v1/2020.emnlp-demos.4. URL <https://aclanthology.org/2020.emnlp-demos.4>.
- [167] Oscar Venter, Eric W. Sanderson, Ainhoa Magrach, James R. Allan, Jutta Beher, Kendall R. Jones, Hugh P. Possingham, William F. Laurance, Peter Wood, Balázs M. Fekete, Marc A. Levy, and James E. M. Watson. Sixteen years of change in the global terrestrial human footprint and implications for biodiversity conservation. *Nature Communications*, 7(1): 12558, August 2016. ISSN 2041-1723. doi: 10.1038/ncomms12558. URL <https://www.nature.com/articles/ncomms12558>. Number: 1 Publisher: Nature Publishing Group.
- [168] O. Venter, E.W. Sanderson, A. Magrach, J.R. Allan, J. Beher, K.R. Jones, M.A. Levy, and J.E. Watson. Last of the Wild Project, Version 3 (LWP-3): 2009 Human Footprint, 2018 Release, 2018. URL <https://sedac.ciesin.columbia.edu/data/set/wildareas-v3-2009-human-footprint>. Type: dataset.
- [169] Stephen E. Fick and Robert J. Hijmans. WorldClim 2: new 1-km spatial resolution climate surfaces for global land areas. *International Journal of Climatology*, 37(12):4302–4315, 2017. ISSN 1097-0088. doi: 10.1002/joc.5086. URL <https://onlinelibrary.wiley.com/doi/abs/10.1002/joc.5086>. [_eprint: https://onlinelibrary.wiley.com/doi/pdf/10.1002/joc.5086](https://onlinelibrary.wiley.com/doi/pdf/10.1002/joc.5086).
- [170] Marcel Buchhorn, Bruno Smets, Luc Bertels, Bert De Roo, Myroslava Lesiv, Nandin-Erdene Tsendbazar, Martin Herold, and Steffen Fritz. Copernicus Global Land Service: Land Cover 100m: collection 3: epoch 2015: Globe, September 2020. URL <https://zenodo.org/record/3939038>. Type: dataset.
- [171] Ashish Vaswani, Noam Shazeer, Niki Parmar, Jakob Uszkoreit, Llion Jones, Aidan N Gomez, Łukasz Kaiser, and Illia Polosukhin. Attention is All you Need. In *Advances in Neural Information Processing Systems*, volume 30. Curran Associates, Inc., 2017. URL <https://proceedings.neurips.cc/paper/2017/hash/3f5ee243547dee91fbd053c1c4a845aa-Abstract.html>.
- [172] Cédric Villani. *Optimal Transport*, volume 338 of *Grundlehren der mathematischen Wissenschaften*. Springer Berlin Heidelberg, Berlin, Heidelberg, 2009. ISBN 9783540710493 9783540710509. doi: 10.1007/978-3-540-71050-9. URL <http://link.springer.com/10.1007/978-3-540-71050-9>.
- [173] Dan Hendrycks and Kevin Gimpel. Gaussian Error Linear Units (GELUs), July 2020. URL <http://arxiv.org/abs/1606.08415>. arXiv:1606.08415 [cs].
- [174] Ondřej Cífka and Antoine Liutkus. Black-box language model explanation by context length probing, December 2022. URL <http://arxiv.org/abs/2212.14815>. arXiv:2212.14815 [cs].

- [175] Leo Breiman. Random Forests. *Machine Learning*, 45(1):5–32, October 2001. ISSN 1573-0565. doi: 10.1023/A:1010933404324. URL <https://doi.org/10.1023/A:1010933404324>.
- [176] Aaron Fisher, Cynthia Rudin, and Francesca Dominici. All Models are Wrong, but Many are Useful: Learning a Variable’s Importance by Studying an Entire Class of Prediction Models Simultaneously. *Journal of Machine Learning Research*, 20(177):1–81, 2019. ISSN 1533-7928. URL <http://jmlr.org/papers/v20/18-760.html>.
- [177] Giles Hooker, Lucas Mentch, and Siyu Zhou. Unrestricted permutation forces extrapolation: variable importance requires at least one more model, or there is no free variable importance. *Statistics and Computing*, 31(6):82, October 2021. ISSN 1573-1375. doi: 10.1007/s11222-021-10057-z. URL <https://doi.org/10.1007/s11222-021-10057-z>.
- [178] Pascal Marchand, Mathieu Garel, Gilles Bourgoïn, Antoine Duparc, Dominique Dubray, Daniel Maillard, and Anne Loison. Combining familiarity and landscape features helps break down the barriers between movements and home ranges in a non-territorial large herbivore. *Journal of Animal Ecology*, 86(2):371–383, 2017. ISSN 1365-2656. doi: 10.1111/1365-2656.12616. URL <https://onlinelibrary.wiley.com/doi/abs/10.1111/1365-2656.12616>. _eprint: <https://besjournals.onlinelibrary.wiley.com/doi/pdf/10.1111/1365-2656.12616>.
- [179] Marlee A. Tucker, Katrin Böhning-Gaese, William F. Fagan, John M. Fryxell, Bram Van Moorter, Susan C. Alberts, Abdullahi H. Ali, Andrew M. Allen, Nina Attias, and Tal Avgar. Moving in the Anthropocene: Global reductions in terrestrial mammalian movements. *Science*, 359(6374):466–469, 2018. Publisher: American Association for the Advancement of Science.